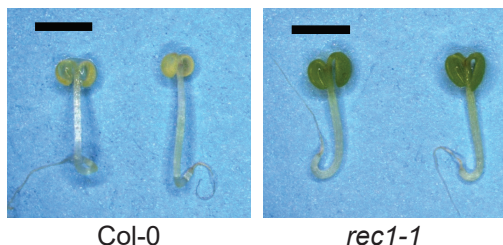
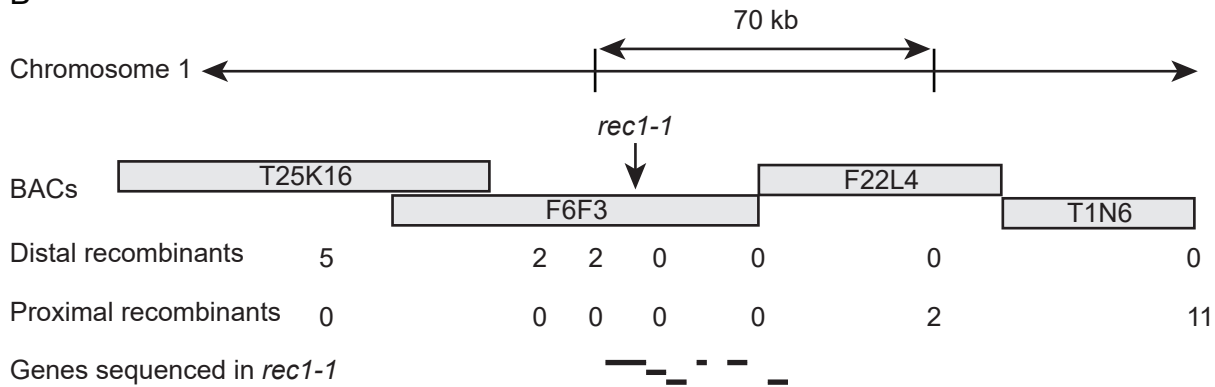


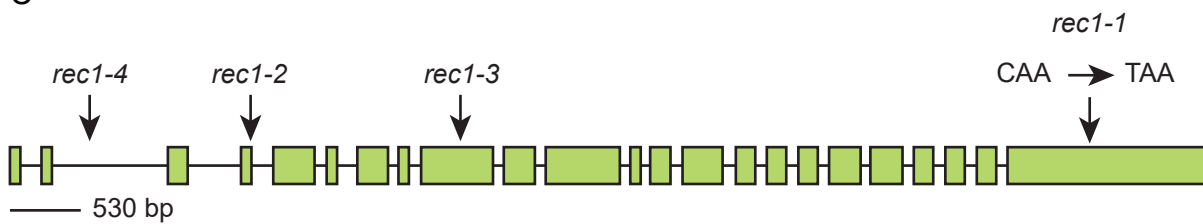
A



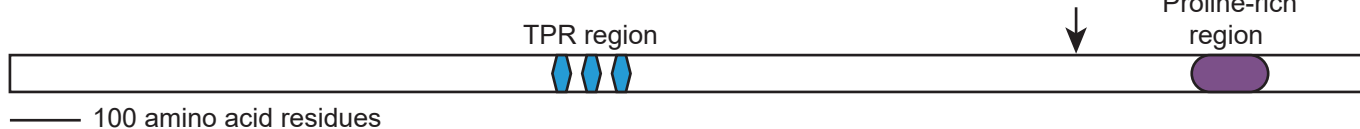
B



C



D

**Fig. S1.** Positional cloning of *rec1-1*.

(A) Inhibition of the far-red block of greening by *rec1-1*. A far-red block of greening experiment was performed as described in SI Materials and Methods. Representative wild-type seedlings (Col-0) that did not green and representative *rec1-1* seedlings that did green are shown. Bar=2mm.

(B) Fine-mapping of *rec1-1*. The absence of the far-red block of greening phenotype in *rec1-1* was fine mapped to a 70 kb interval based on an analysis of 2376 chromosomes from F2 progeny derived from a cross of *rec1-1* and the recombinant inbred lines described in SI Materials and Methods. Chromosomes were analyzed using SSLP, CAPS and dCAPS markers (Supplemental Table S3) that were derived from the indicated bacterial artificial chromosome clones (BACs). The number of centromere proximal recombinants (Proximal recombinants) and centromere distal recombinants (Distal recombinants) that were identified with each marker are indicated. The relative positions are indicated for seven genes in the 70 kb interval that were sequenced.

(C) Mutant alleles of *REC1*. Boxes and lines indicate translated exons and introns, respectively. The mutated codon in *rec1-1* is indicated. The positions of the T-DNA insertions in *rec1-2* (SAIL_555_D11), *rec1-3* (Salk_049453) and *rec1-4* (Salk_132306) are indicated with arrows.

(D) Diagram of the REC1 protein. The REC1 protein is indicated with a white box. The TPR region, Q1415 and the proline-rich region are indicated.

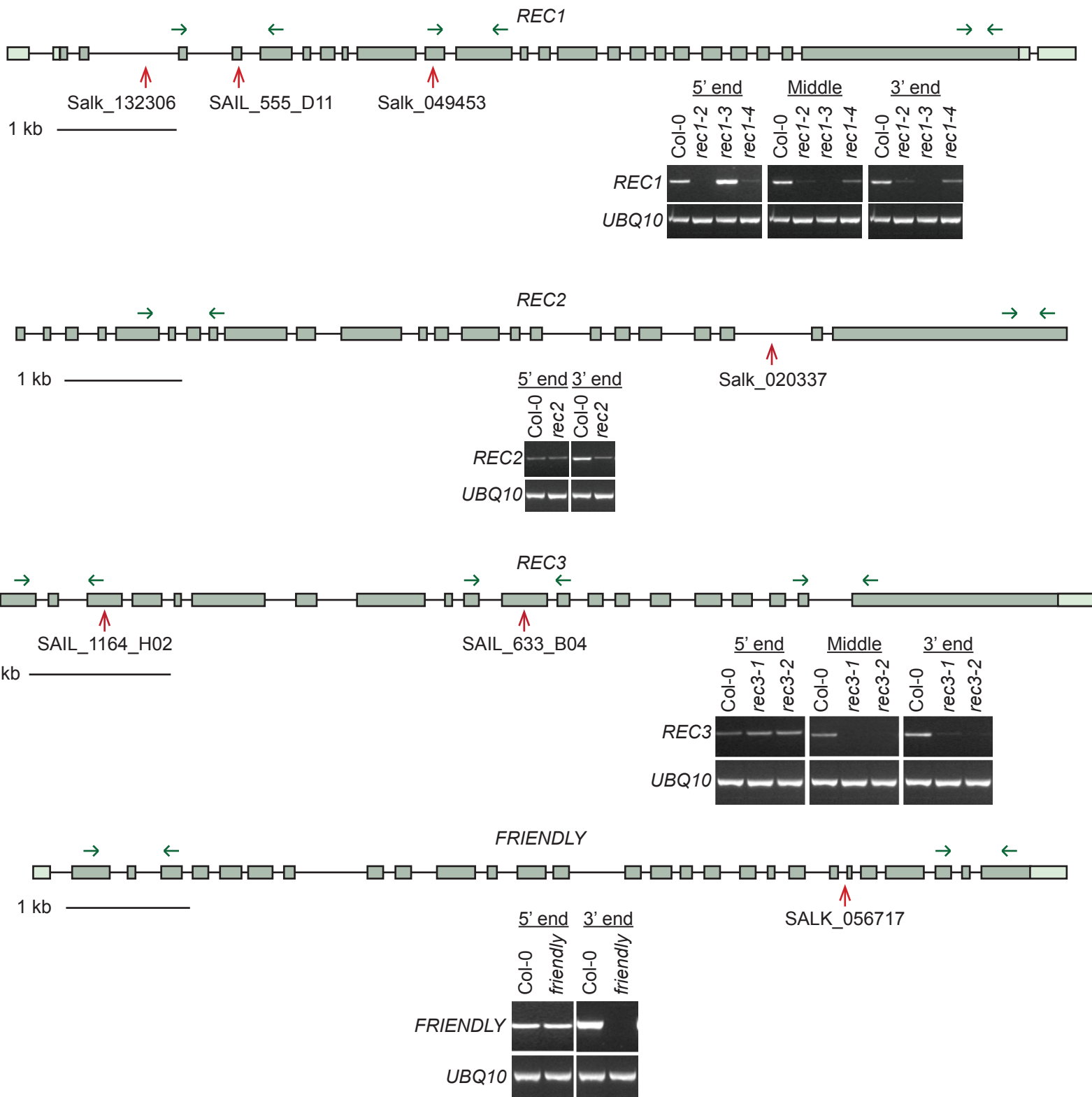


Fig. S2. RNA phenotypes of *REC1*, *REC2*, *REC3* and *FRIENDLY* T-DNA insertion mutants.

The gene diagrams for *REC1*, *REC2*, *REC3* and *FRIENDLY* indicate the translated exons (dark-green boxes), untranslated exons (light-green boxes), and introns (black lines). The positions of T-DNA insertion sites are indicated with red arrows. The primer binding sites are indicated with green arrows. Relative levels of mRNA quantified by each pair of primers in wild type (Col-0) and the indicated mutants are shown below each diagram. *UBQ10* expression was analyzed to test whether the same amounts of cDNA were used for each PCR.

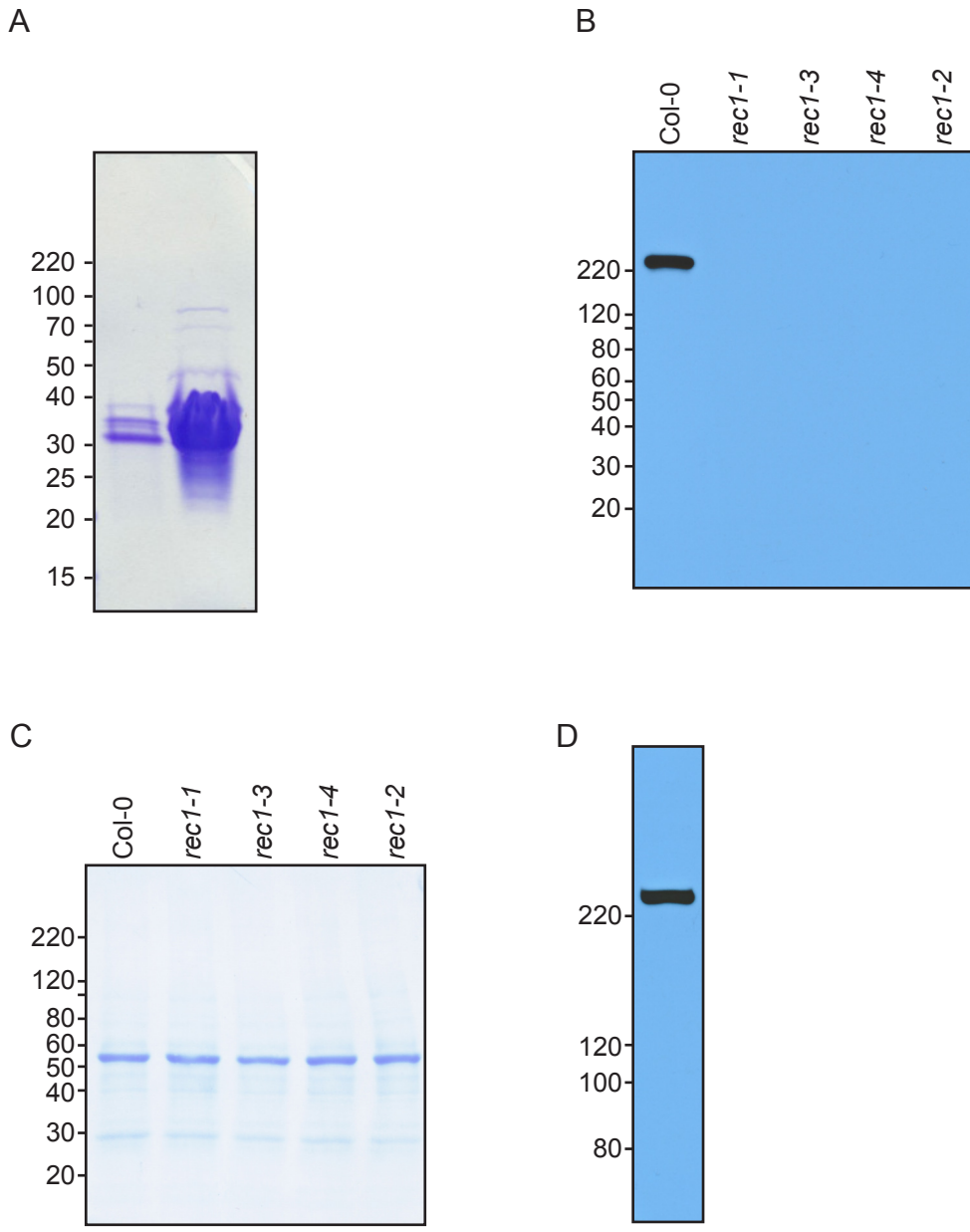


Fig. S3. Characterization of affinity purified anti-REC1 antibodies.

(A) Analysis of purified REC1 fragments. Purified fragments of REC1 derived from residues P1419 to F1673 were analyzed using SDS-PAGE and staining with Coomassie brilliant blue R-250. The two lanes contain 1 µg and 11 µg of protein.

(B) Immunoblotting of whole-leaf extracts from wild type and *rec1* mutants. Whole-leaf extracts were prepared from equal amounts of leaves from 24-d-old plants using denaturing conditions. Equal volumes of extracts from wild-type (Col-0), *rec1-1*, *rec1-2*, *rec1-3* and *rec1-4* were analyzed by SDS-PAGE with a 4 to 20% gradient gel and immunoblotting using affinity-purified anti-REC1 antibodies. The mass of each standard protein is indicated at the left in kDa.

(C) Total protein analysis of the immunoblot from (B). After immunoblotting, the polyvinylidene fluoride membrane was stained with Coomassie brilliant blue R-250. The mass of each protein standard is indicated at the left in kDa.

(D) Immunoblotting of a whole-leaf extract from wild-type. The whole-leaf extract described in (B) was analyzed by SDS-PAGE with a 5% gel and immunoblotting as described in (B). The mass of each standard protein is indicated at the left in kDa.

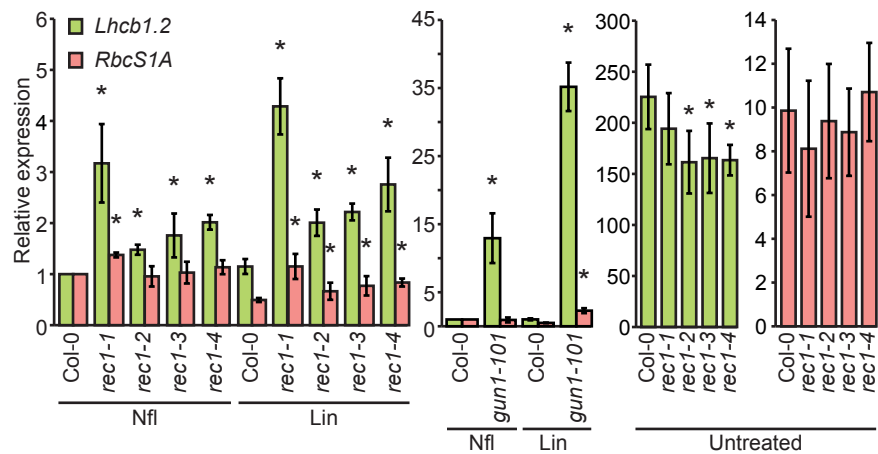


Fig. S4. Plastid-regulated expression of *Lhcb1.2* and *RbcS1A* in *rec1* mutants and *gun1-101*. Chloroplast biogenesis was blocked by growing seedlings on media that contained either norflurazon (Nfl) or lincomycin (Lin). Seedlings containing chloroplasts were grown on a medium containing no inhibitor of chloroplast biogenesis (untreated). Four biological replicates were analyzed for wild type (*Col-0*) and each mutant in each condition. Expression is reported relative to wild type (*Col-0*) treated with norflurazon, which is assigned a value of 1. Error bars represent a range calculated with the equation $2^{-\Delta\Delta CT \pm \text{standard deviation}}$. * indicates a statistically significant difference relative to wild type (*Col-0*) grown on the same medium ($P < 0.0001$ to 0.047).

REC1	MAPKNNNRGK-----TKGDKKKKKEEKVL-PVITVDIVIVNLP-----	33
REC2	MAPKAGKTKPHK-----SKGEKKKKKEEKVL-PTVIEISVETP-----	36
REC3	MAFRSSSKGKSNNKG---KGGDKKKRDKKLAPSLEITVTTP-----	39
FRIENDLY	MAGKSNSKSKAKRAAQSTTNSTTDVKSDAPAPPVAATVPATAPVTAAAAPVATAAAPVTAPDNGTLTAVD	70
REC1	-----DETEAILKGIST-----DRIIDDVRRRLLSVN	58
REC2	-----DESQVTLKGIST-----DRILDVVRKLLAVH	61
REC3	-----YETQVILKGVST-----DKIIDDVRRLLASH	64
FRIENDLY	SAVPEANEVAPTIKPKADESESQVENNDAAQPKQGELRLYPVSVKTQSGGKMEQLQLNPGDSVMDIRQFLLDA	140
REC1	FDTCHVTNYSLSHIRG---SRLKDTVDVSAIJKP-----CVLTLTEEDY-NEGTAVAHVRRLLDIVACTT	119
REC2	VQTCFTNFSLSHQVRG---TKLKDSVDIVSLKP-----CHLTIVEEDY-TEEQATAHTIRRLLDIVACTT	122
REC3	VETCHFTNYSLSHKVKG---HKLNNDIQVQLSLKP-----CFLRMIPEEYLEESQALTQVRRVIDIVACTT	126
FRIENDLY	PETCYFTCYELLRNKDGETHHLEDYNEISEVADITIGGSLEMVAALY-DDRSIRAHVHRARDLLSLST	209
REC1	CFGPS-----PEKSDSVKSAQVKGGGKNQSDT-----SPPSPASKDVT-----VDEAGETS	168
REC2	AFGPSKPPVSRTLPKDSEKKESGSTDGDSPTEKDAGDSNSGLSPKPESEKKSVGACEAQSAEGAAKSDI	192
REC3	RF-----FSKSPNKSIVAGNA-----NPTPAFDGLDMV-----AI	156
FRIENDLY	LHSSL-----STTLALQYDAALNKVQNPGD-----KPKSDVPELECLGFMEDV--PGSLKKLI	260
REC1	HSFP--KLGSFYEFFSLAHLTPPLQYIRLATKRETEDIAKEDHLLSIDVKLCNGKLVHIEGCRKGFY---	233
REC2	DMCPPTRLGOFYEFFSFYLTTPPIQYIRRSPRKEDKGDD-LFQIDIKVSSGKPFITVVASRTGFY---	258
REC3	HTTP--KLSQFYEFFSIHLSPPPIHLKKVDPGEAGEKRDGD-YFGLKVKICNGKVIHVIAVKGF---	220
FRIENDLY	NSTS--EEIRSVENIVFSSFNPPPSHRRLV-----GD-LIYLDVVTLEGNKYCITGTTKTFYVNS	317
REC1	-----SIGKQRIICHNLVDLIRQISRAFDNAYSDLILKAFSERNKFGNLPYGFRANTWL-----IPPTA	291
REC2	-----PPGKQQLLCHSLVELLQQISRPFDAAYDALMKAFIEHNKFGNLPYGFRANTWV-----VPPVV	316
REC3	-----AVGKQLSHCHSIVDLLQNVSNAFAKAYESLMKAFTDRNKFGNLPFGLRSNTWL-----VPSPV	278
FRIENDLY	SSGNILDPRSKSGFEAATLIGLLQKLSSKFKAFAREVMEKKASAHPENVQSLIIPPHSWLRTYPVPDFHK	387
REC1	AQSPAAPPLPVEDERWGGDGQQGRDGSYDLVPWSNEFAFIASMPCKTAERQVRDRKVFLHLNLFVDV	361
REC2	ADSPSTFPSLPVEDET WGGDGQQGRDGSYDLVPWSNEFAFIASMPCKTAERQVRDRKVFLHLNLFVDV	386
REC3	SESAS---PLPTEDEHWGGNGGGQGRNGEYDHWRPAAAEFSVLATLPCKTEERVIRDKKAFLLHSQFIDT	345
FRIENDLY	RDAARAAEALTI--SYGSELIGMQRD-----WNEELQSCREFPHTSPQERILRDRALYKVSSDFVDA	447
REC1	ATFRAIKAVQVMAEPVLAED----SEVLYSETVRDLTVTVTRDTSNASSK-----	409
REC2	SVEKAVEIIKKIVENNQCSLKD---PAALGFHEERIGDLIVRVARRDDPASAK-----	436
REC3	SVORAVRAICNVMDTNQQTSGTTDLPAGSILLEDHVGDLSIVVKRDIASLDISK-----	398
FRIENDLY	ALNCAIGVISRCI--PPINPTD---PECLHMYVHNНИFFSAVDADIEQLSKRPSONQMTEKVSSSEKVS	512
REC1	-VDTKIDGIQATGLDKKKLME-----RNLLKGLTADENTAAHDVATLGTISLKYCGYIAVVKLEKE	469
REC2	-LDRKSDGTQVLEISQEELAQ-----RNLLKGITADESATVHDTSTLGVVVVRHCGCTAVKVASE	496
REC3	-PHEATFQN-DAFVLSSSEELAE-----RNLLKGITADESVI VHDTPALGKVIVRQCGYTAVVNVKGQ	457
FRIENDLY	CTEGTCDNEEHNNCNEAPLIVENEQATYASANNDLKGTKLYQEADVPGILYNLAMAIIDYRGHRVVAQ--SV	580
REC1	SEELSPPSQIVDLL--EQPEGGANALN-----INSLRFLLHKSSPEQNKK-----TPQOHD-DELT	522
REC2	F-KLNDGHILQDIDIEDQSEGGAANLN-----VNSLRTLLHKSTPSSLQ-----SP-NADSEQIR	552
REC3	TQKAM--SDFRDILIDDLIPDGGGANLN-----LNSLRVEFHRPHSGVTSVEN-----QPTQLDWDDLE	513
FRIENDLY	LPGILQGDKS DALLYGSVDNGKKICWNEDFHAKVLEAAKLLHIKEHSVIDASSETVFKLAAPVECKGIVGS	650
REC1	SSREFVSKMLEESIAKLEGE-EIDRDSIMRWELGACWIQHLQDQKNTEDKKQTKGEKSKNELKVEGLGKP	591
REC2	VAKSLVRKVIEDSLKKLEIE-PSRYSKPIRTELGVWVQHQLQNQASSKSESKKT-EDPKPEPAVKGLGKQ	620
REC3	SYRCIIQELVKINLTKEFT-RVSSVRPIRTELGVSTWVQHQLQKKTEDVCGKPAT--NDETELSVKGLGKQ	580
FRIENDLY	DNRHYLLDLMRVT PRDANYTGPESRFCVLRPELITSFCQAESLEKSFKTKADEGGDDSSNVSA DT SKVG	720

REC1	LKSLNSSKKKTDVSSPKTPQTALSSQVDAVSSEADTAASLQSDAEKNAQEENVLILKNLLSDAAFTRLIKES	661
REC2	GALLKEIKRKIDVKANKTEQ---GKEAPANDTDNTSETEDQKELEKQNEEIEKMWKEIVTETAYQRLIKES	687
REC3	FKDLKSkskkskSENISAVNEK-----DTRLHELNNEEDLGQKSIDGLFTELKELLSEEAFSRLKET	640
FRIENDLY	DALIDGEANGASNSDQKSI-----DKQNTTAEDYAAAGSSESSKSCDQIA-----FNPNVFTDFTLG	777
REC1	DTGLHHKSLQELVLDIAQNYYTEVAIIPKLVADFGSLELSPVDGRTLTDFMHTRGLRMRSLGYVVKLSDKLS	731
REC2	ETGFHLKSPKELIEMARKYYTDTALPKLVADFGSLELSPVDGRTLTDFMHTRGLQMHSLGRVVELAEKLP	757
REC3	GTGLHLKSKELTNMAYGYYDEIALPRLVADFGSLELSPVDGRTLTDFMHIRGLQMRSLGHVAKLAEKLP	710
FRIENDLY	GNQEEIAADEENVKKVSSYLVDDVLPKFIEDLCTLEVSPMDGQTLTEALHAHGKVNVRYIGRVANGVKHLP	847
REC1	HVQSLCVHEMIVRALKHILQAVISAVATDTDKIAIKVAAALNMMLGI--PENVAATPHNPWNVHP-----	794
REC2	HVQSLCVHEMIVRAYKHILQAVVAAV-ENTADVATSIAATCLNVILLGT--PSDTESVYDEK-----	814
REC3	HVQSLCIHEMITRAFKHILRAVIASV-NNMAELPVAVAASLFNMLGRRELEGCDRIPGEEYC-----	771
FRIENDLY	HLWDLCLNEITVRSAKHILKDILRDI-EDHD-IGSAVSHFLNCFFGNYQTAGGKASANSSTAKNQKKDQP	915
REC1	-----LIFRWLEKFLKKRYDYDLNAFSYKDLRKFAILRGLCHKVGIE	836
REC2	-----IKWTWVETFISKRFGWDWKHEGCQELRKFSILRGLSHKGLE	856
REC3	-----LRLQWLQKFLSRKFGW-IQKDEFHHLKKFSILRGLCQKVGLE	812
FRIENDLY	ITKKKGQGRGKGKASSKKSFSSYMMVDSNIIWSDIQEFAKAKYEFELPELSRTTAKKVSVLRNLCQKVGS	985
REC1	LIPRDFDMDSAPPFRKTDVVSLVPVHKTFYFKSMQQAACSSADGRQLLESSKTA	906
REC2	LVPKDYEMDTSYPEKKFDIISMVPVYK-----HVACSSADGRTLLESSKTS	918
REC3	LVSRRDFDFDSPNPFMSSDIIGLVPVCK-----HVLCISSLGRTLLESSKIALDKGKLDLDAVSYGTKA	874
FRIENDLY	IAARKYDFSANTPFETSDILDILRPVIK-----HSVPCSEAKDLVEMGKVQLAEGMISESYTFFSEA	1047
REC1	LAKLVAVCGPYHRMTAGAYSLAVVLYHTGDFNQATIYQQKALDINERE	976
REC2	LAKLVAVCGPYHRMTAGAYSLAVVLYHTGDFNQATIYQQKALDINERE	988
REC3	LVKMIAVCGPYHRNTACAYSLLAVVLYHTGDFNQATIYQQKALDINERE	944
FRIENDLY	FSILOQVITGPMPREVANCCRYLAMVLYHAGDMAGAIMOQHKELI	1117
REC1	-----LQHTELALKYVKRALYLLHTCGPSHPNTAATYINVAMMEEGLGNVHVALRYLHKALKCNQRLLGPDHIQ	1046
REC2	-----LQHTELALKYVNRALYLLHTCGPSHPNTAATYINVAMMEEGMKNAHVALRYLHEALKCNQRLLGADHIQ	1058
REC3	-----LQHFELALKYVNRAFLFLHFTCGLSPHPNTAATYINVAMMEEKEVGNDHLLALRYLHEALKSNKRLLGADHIQ	1014
FRIENDLY	LNQTELALQNMGRAILLLGLSSGPDPDVAAATFINVAMMYQDMGKMDTALRYIQEALKKNERLLGPEHIQ	1187
REC1	TAASYHAIAIALSLMEAYHLSVQHEQTTIIRILRAKLGPDLLRTQAAA	1116
REC2	TAASYHAIAIALSLMDAYSLSVQHEQTTIQLQIAKLGPEDLRTQAAA	1128
REC3	TAASYHAIAVALSFMEAHSLSVQHEQTTIQLITA	1084
FRIENDLY	TAVCYHALAIAFNCGAFKLSHQHEKKTYDILVKQLGDDDSRTRDSLNWMKTFKMRELQMTAQKQKG--	1254
REC1	PDAISASKGHLSVSDL	1186
REC2	PDAISISSKGHLSVSDL	1186
REC3	PDAISASKGHLSVSDL	1139
FRIENDLY	-----	1254
REC1	DTEETGSEE	1252
REC2	EILSPAHLTGESSSDKENKSETKSEEKK-----VENFDI	1251
REC3	RVASQIDIVTWNNVAEADVTKSRS	1206
FRIENDLY	-----QAANAANTQKAIDL	1271
REC1	-QRPRSAGSYGRRMKQR	1320
REC2	-V-PKNRFSSGRRT-----RPSLA	1300
REC3	YSKGRSGNGAGRKSQRQ	1252
FRIENDLY	-----HPDLIH-----AFQNAAA-----TGRTNALNS-----	1293

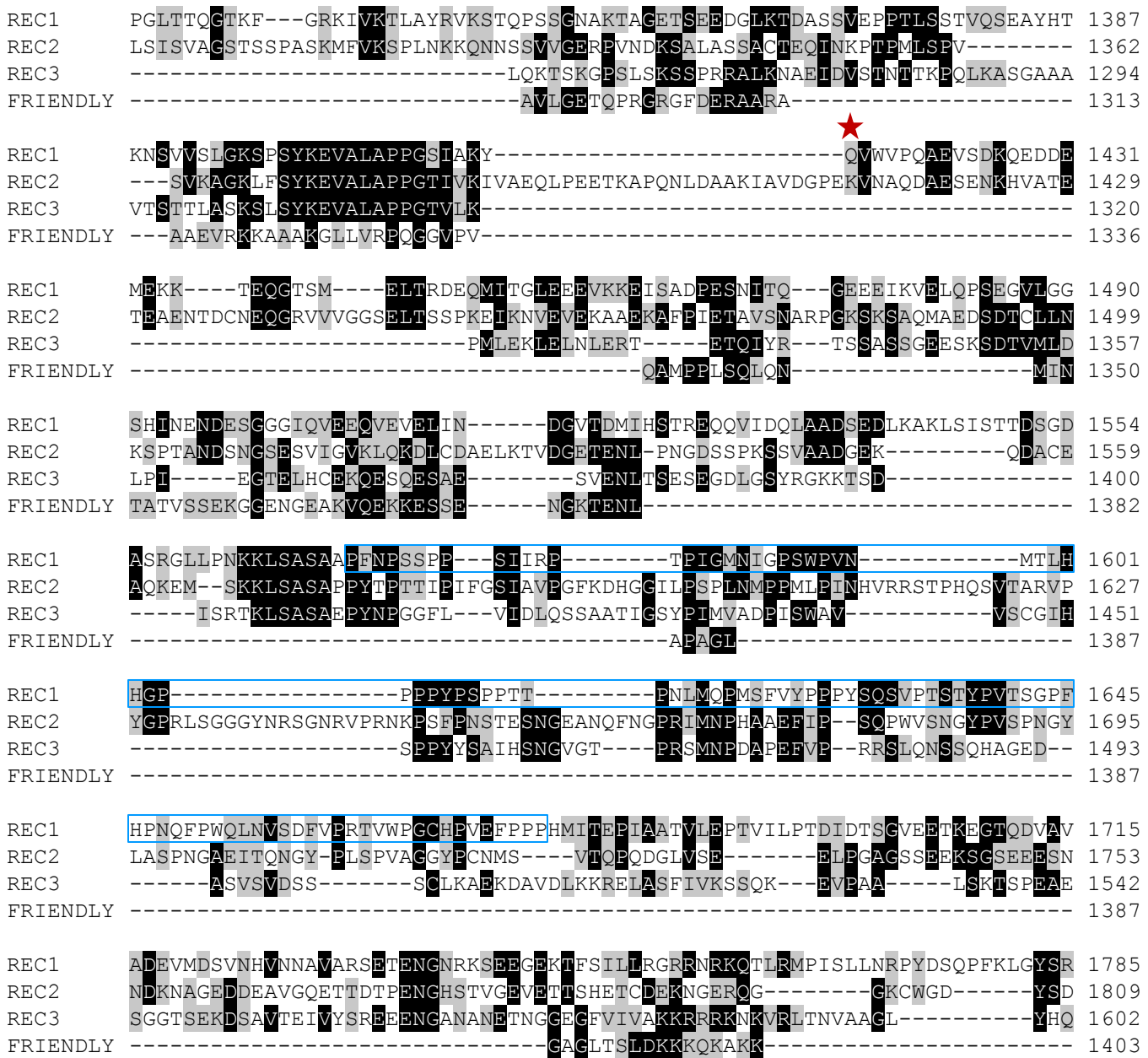


Fig. S5. Sequence similarities among REC1, REC2, REC3 and FRIENDLY. Identical amino acids are shaded with black boxes. Similar amino acids are shaded with gray boxes. The tetratricopeptide repeats are indicated with red boxes. Q1415 is indicated with a red star. The proline-rich region of REC1 is indicated with a blue box.

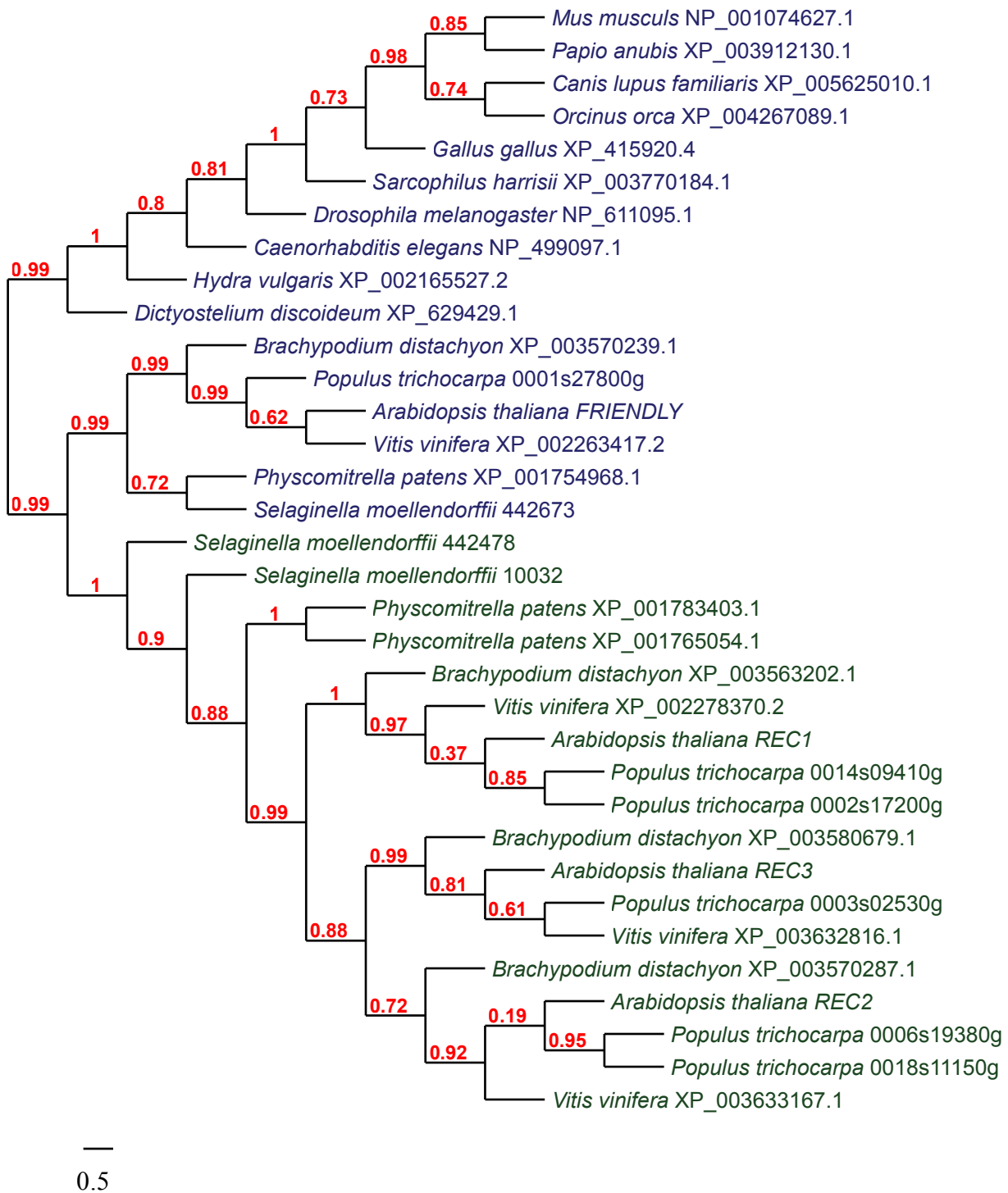


Fig. S6. Phylogeny of amino acid sequences homologous to REC1. Sequences are represented by the name of the organism and a number assigned to the particular amino acid sequence, such as the NCBI reference sequence number. Sequences that are more closely related to FRIENDLY are indicated with blue text. Sequences that are more closely related to REC1, REC2 and REC3 are indicated with green text. Bootstrap values are indicated with red numbers.

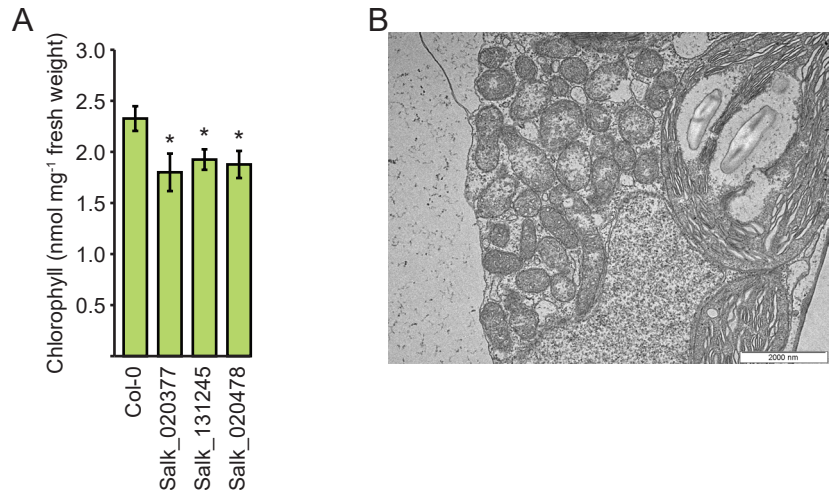
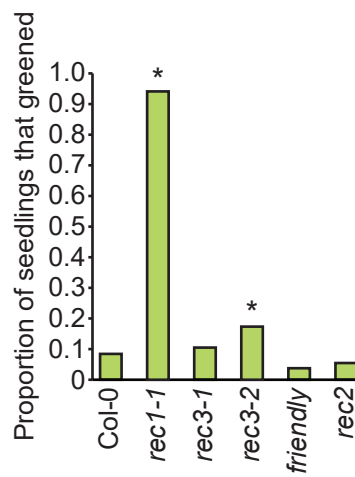


Fig. S7. Characterization of *rec2* and *friendly* mutants.

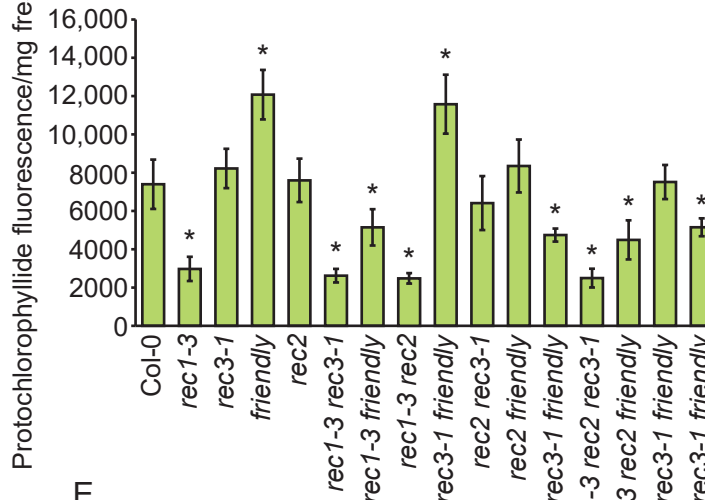
(A) Chlorophyll-deficient phenotypes of *REC2* mutants. The plants were grown in soil for 23 d. Six biological replicates were analyzed for wild type, Salk_020377 and Salk_020478. Four biological replicates were analyzed for Salk_131245. Error bars indicate 95% confidence intervals. * indicates a statistically significant difference relative to wild type ($P=0.0006$ to 0.0017).

(B) TEM analysis of mitochondria from a *FRIENDLY* mutant. A representative transmission electron micrograph shows a cluster of mitochondria that is typical of *FRIENDLY* mutants.

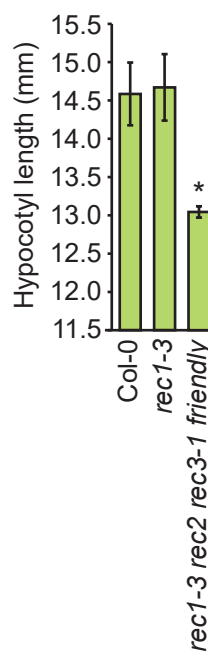
A



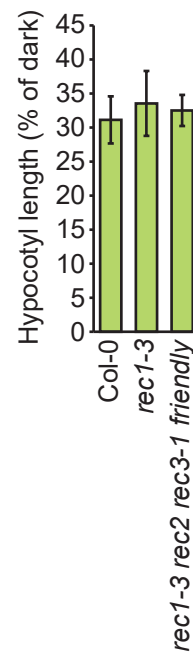
B



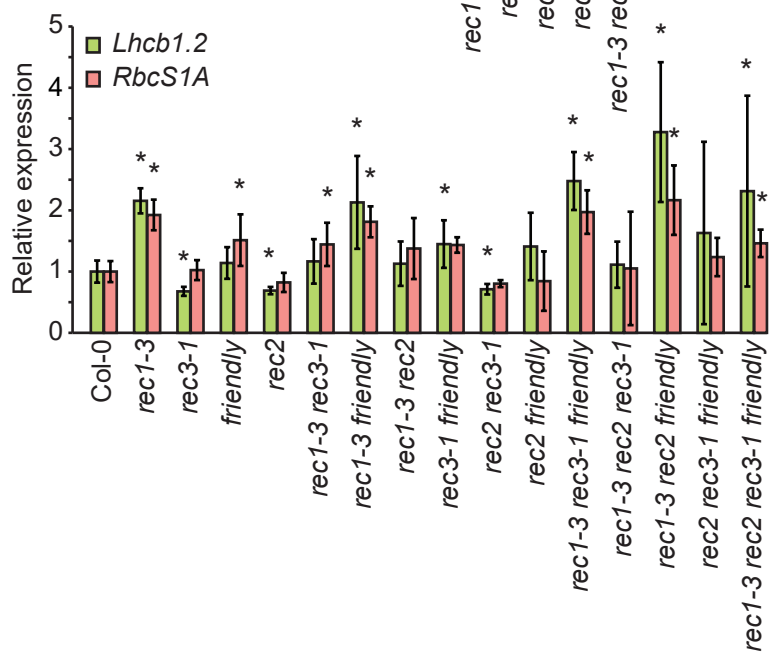
C



D



E

**Fig. S8.** Characterization of *REC* gene family mutants.

(A) Far-red block of greening phenotypes in *REC1*, *REC2*, *REC3* and *FRIENDLY* mutants. A far-red block of greening experiment was performed as described in SI Materials and Methods. The proportions of seedlings that greened are indicated ($N=121\text{-}204$, numbers pooled from three biological replicates). * indicates a statistically significant difference relative to wild type ($P<0.0001$ and 0.03).

(B) Accumulation of protochlorophyllide in *REC* gene family mutants. Seedlings were grown in far-red light as described in SI Materials and Methods. Error bars indicate 95% confidence intervals. * indicates a statistically significant difference relative to wild type (Col-0) ($P=0.0004$ to 0.03).

(C) Hypocotyl lengths of *rec1-3* and *rec1-3 rec2 rec3-1 friendly* grown in the dark. Error bars indicate standard deviation. * is as in (B) ($P=0.0003$).

(D) Hypocotyl lengths of *rec1-3* and *rec1-3 rec2 rec3-1 friendly* grown in far-red light. Hypocotyl lengths in a particular line are presented as a percentage of the average hypocotyl length of that same line grown on the same medium in the dark. Error bars are as in (C).

(E) Plastid-regulated expression of *Lhcb1.2* and *RbcS1A* in the *REC* gene family mutants. Chloroplast biogenesis was blocked by growing seedlings on a medium that contained lincomycin. Expression is reported relative to wild type (Col-0), which is assigned a value of 1. Error bars represent a range calculated with the equation $2^{-\Delta ACT \pm \text{standard deviation}}$. * indicates a statistically significant difference relative to wild type (Col-0) ($P=0.0001$ to 0.045).

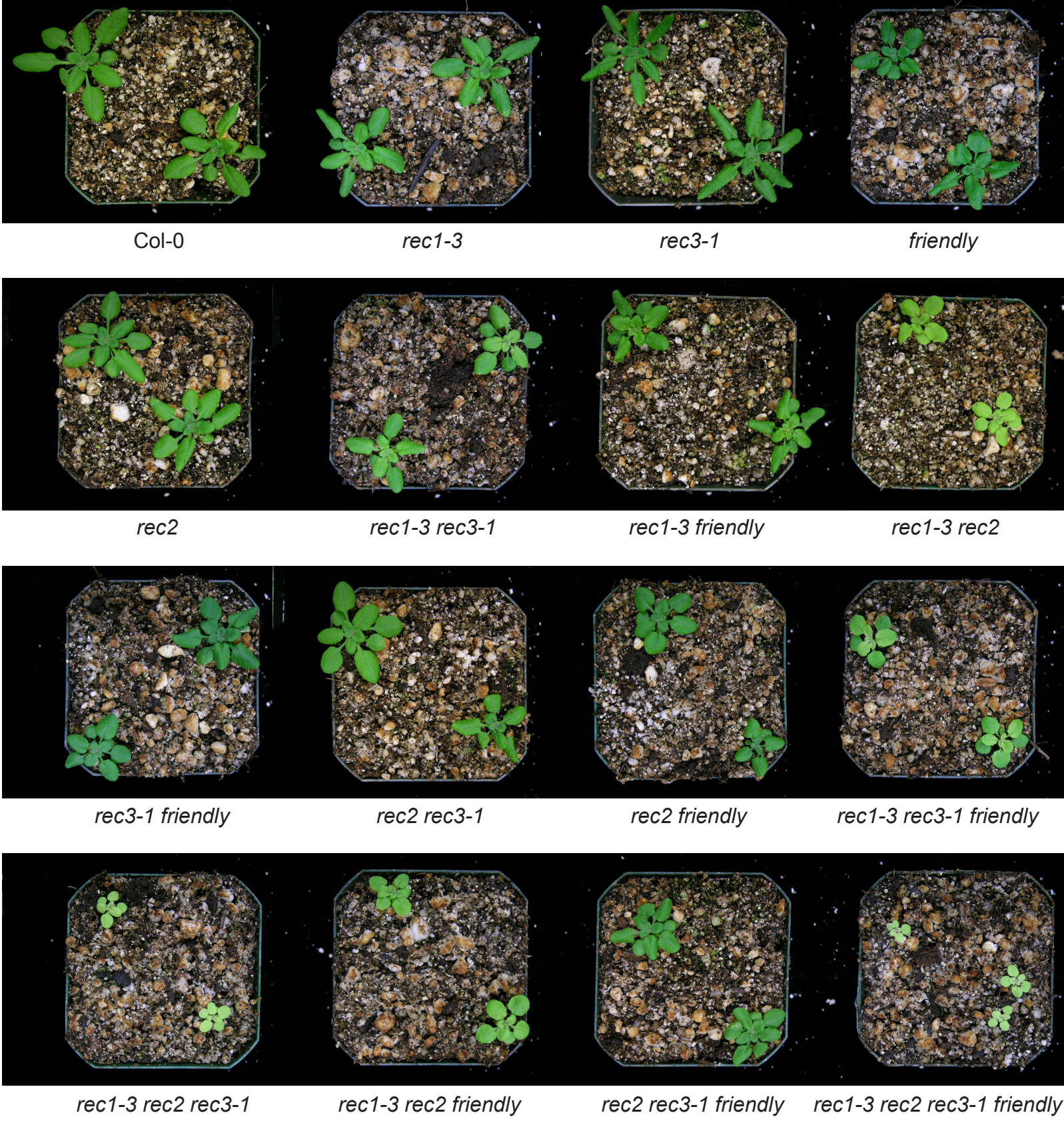


Fig. S9. *REC* gene family mutants. Representative 24-d-old plants are shown.

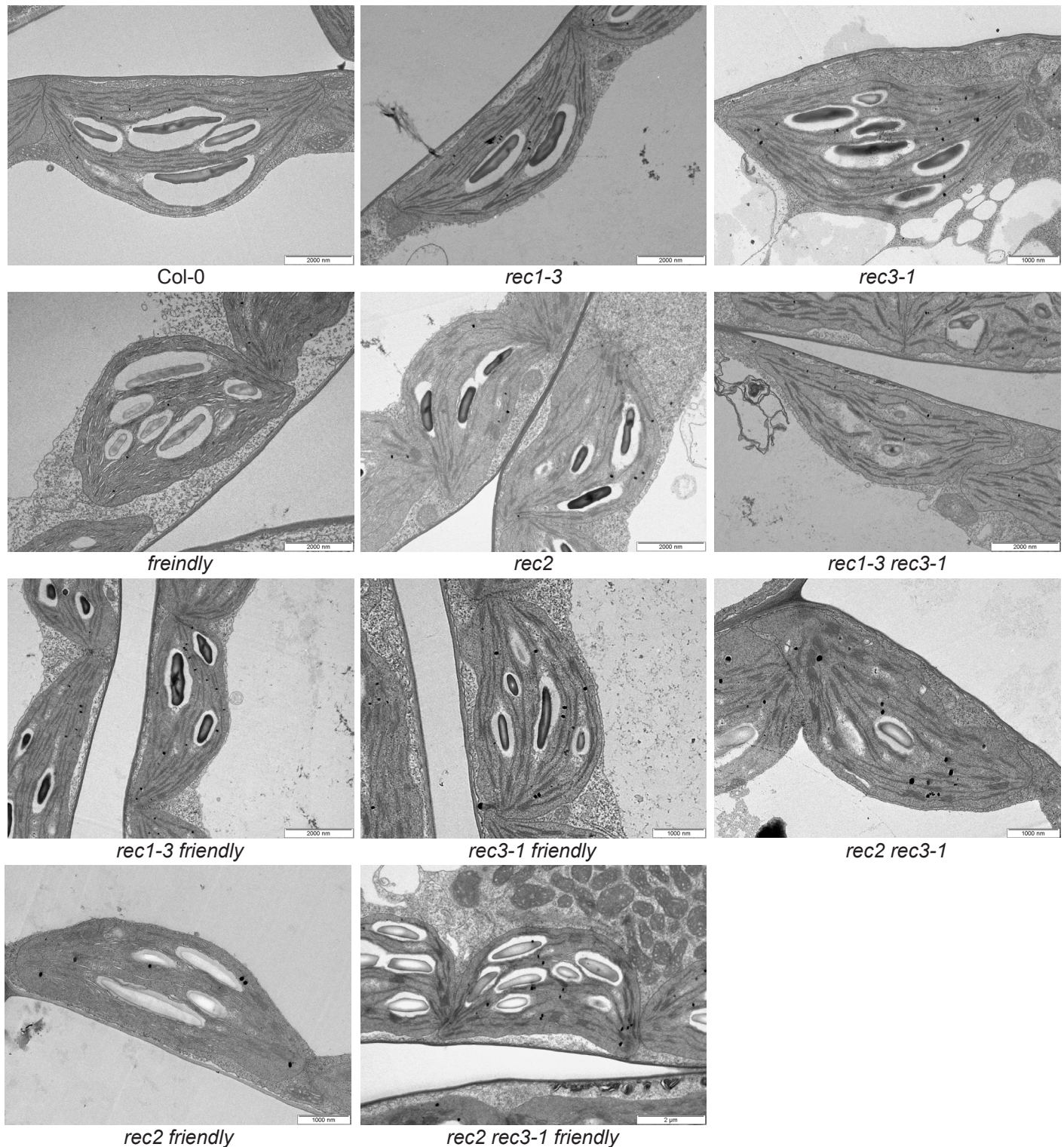


Fig. S10. TEM analysis of chloroplasts from the *REC* gene family mutants that resembled wild. Representative transmission electron micrographs of chloroplasts from 22-d-old wild type (Col-0) and the indicated *REC* gene family mutants are shown.

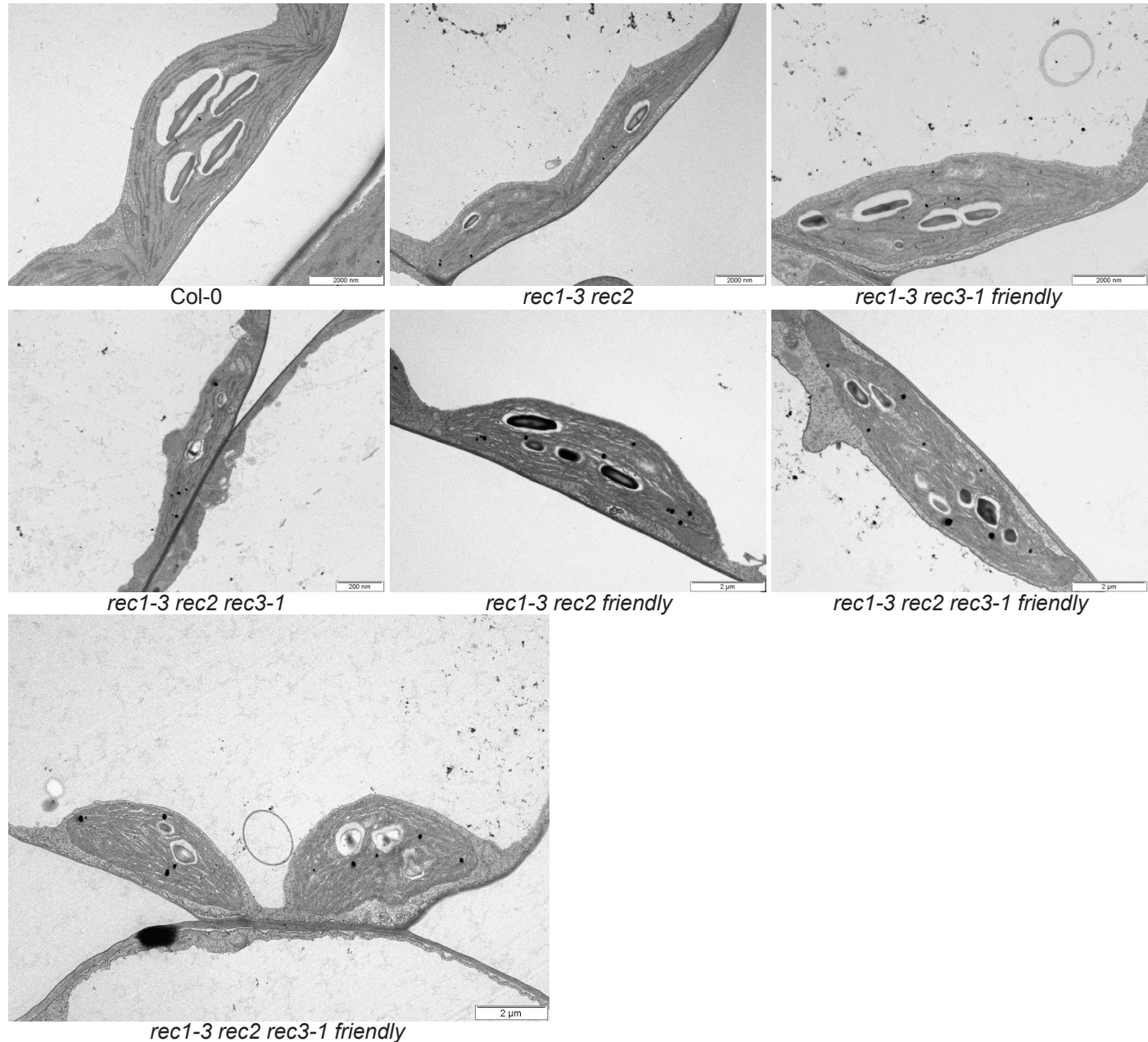


Fig. S11. TEM analysis of chloroplasts from the *REC* gene family mutants that did not resemble wild type. Representative transmission electron micrographs of chloroplasts from 22-d-old wild type (Col-0) and the indicated *REC* gene family mutants are shown.

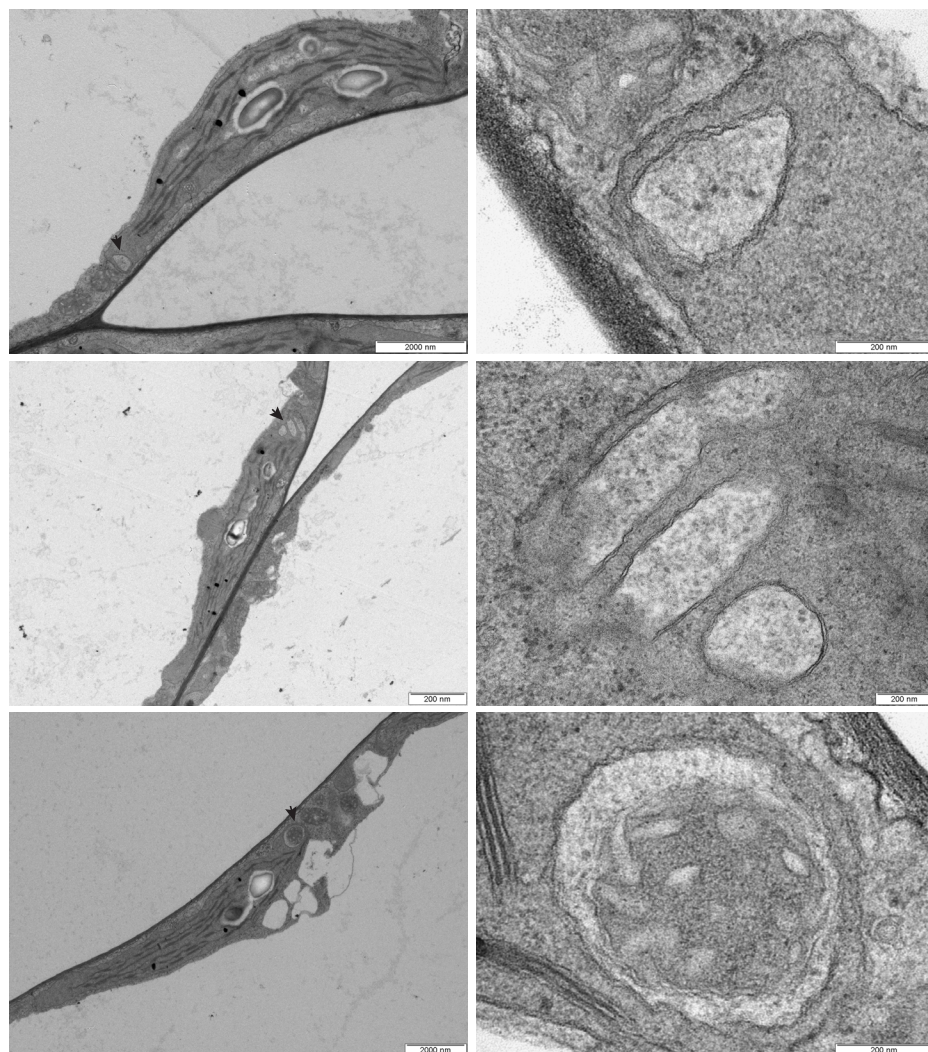


Fig. S12. TEM analysis of cytoplasmic protrusions into the chloroplast stroma in *rec1-3 rec2 rec3-1*. Representative transmission electron micrographs of chloroplasts from 22-d-old *rec1-3 rec2 rec3-1* are shown (left). The positions of cytoplasmic protrusions into the chloroplast stroma are indicated with arrows (left). High magnification micrographs of each chloroplast (right) reveal chloroplast double membranes surrounding each cytoplasmic protrusion. A mitochondrion appears in one of these cytosolic protrusions (lower right).

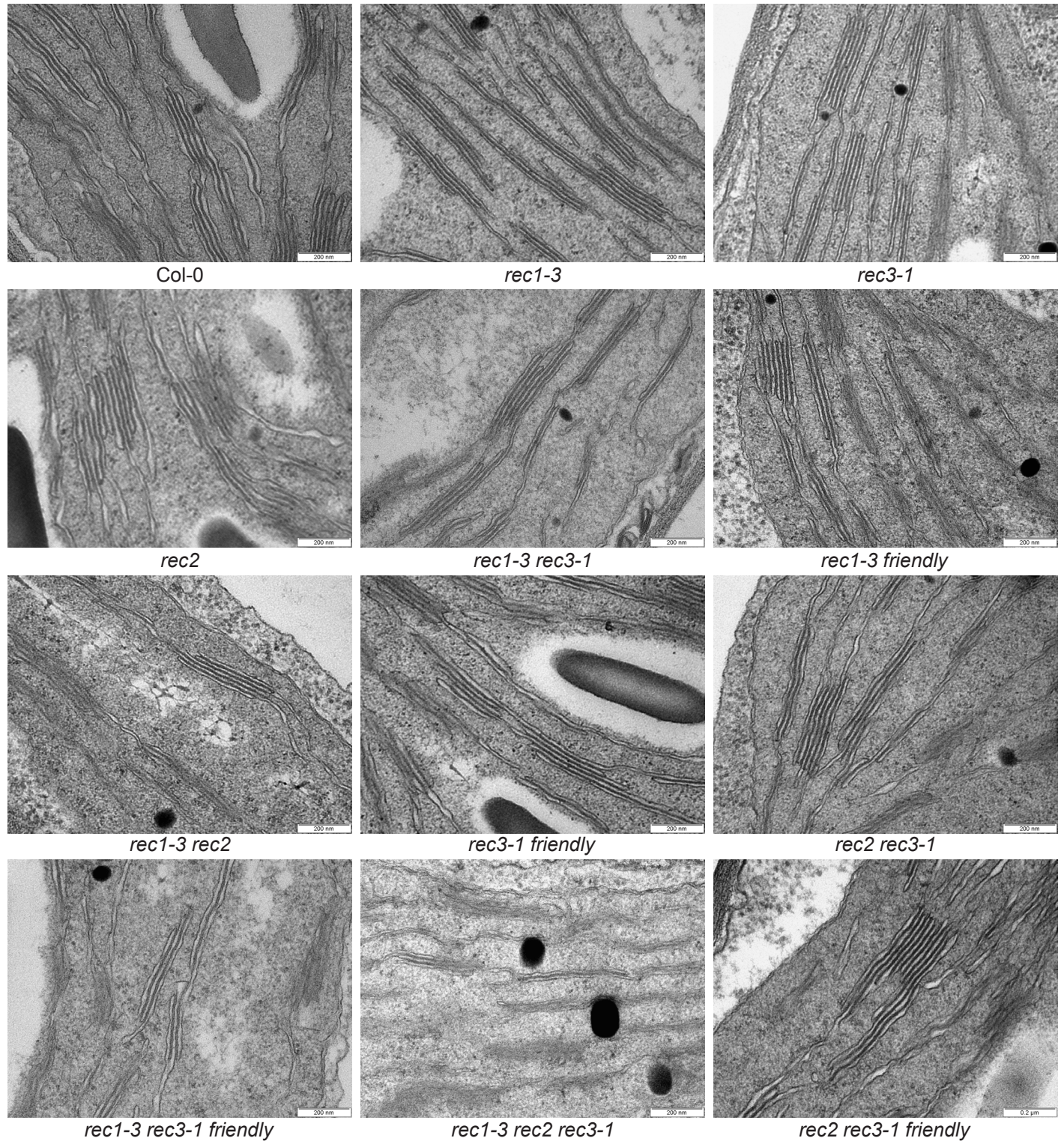


Fig. S13. TEM analysis of thylakoid membranes from the *REC* gene family mutants that appeared similar to wild type. Representative transmission electron micrographs of chloroplasts from 22-d-old wild type (Col-0) and the indicated *REC* gene family mutants are shown.

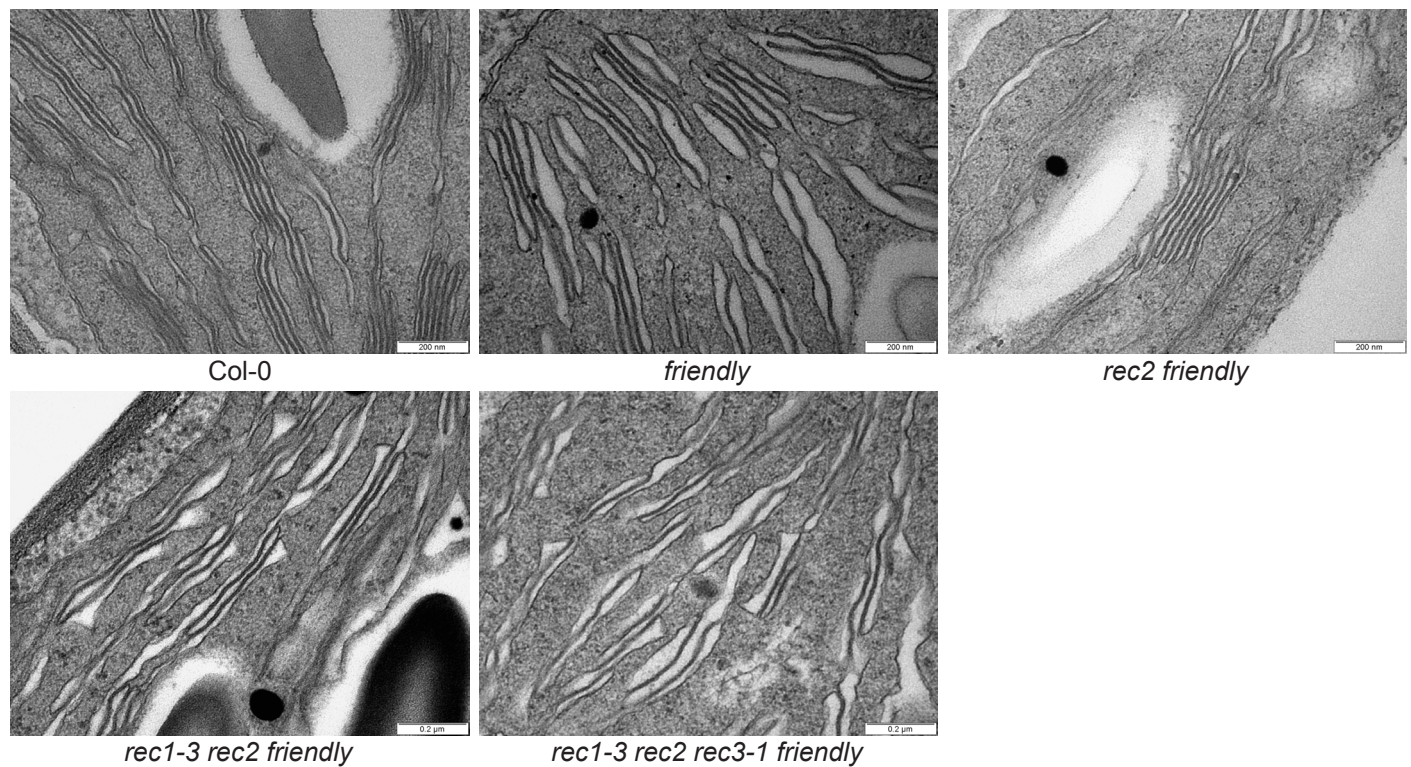


Fig. S14. TEM analysis of thylakoid membranes from the *REC* gene family mutants that appeared swollen relative to wild type. Representative transmission electron micrographs of chloroplasts from 22-d-old wild type (Col-0) and the indicated *REC* gene family mutants are shown.

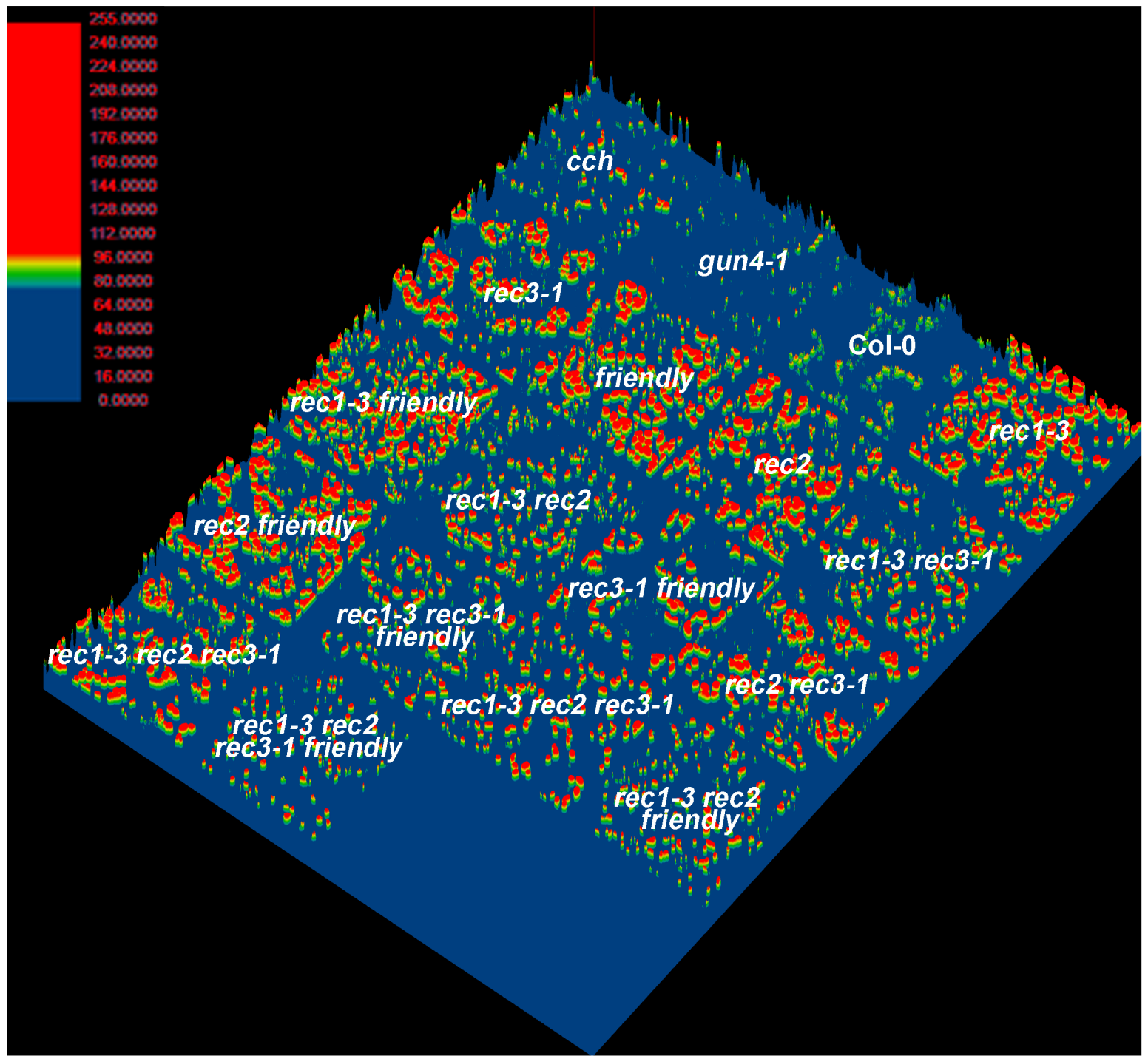


Fig. S15. Chlorophyll fluorescence in the *REC* gene family mutants, *cch* and *gun4-1*. Each surface plot was obtained from the micrographs described in Fig. 3A. Fluorescence intensity increases from blue to red in wild type (*Col-0*) and the indicated mutants. The fluorescence intensity scale is based on a 0–255 RGB color code (0 = minimum intensity; 255= maximum intensity).

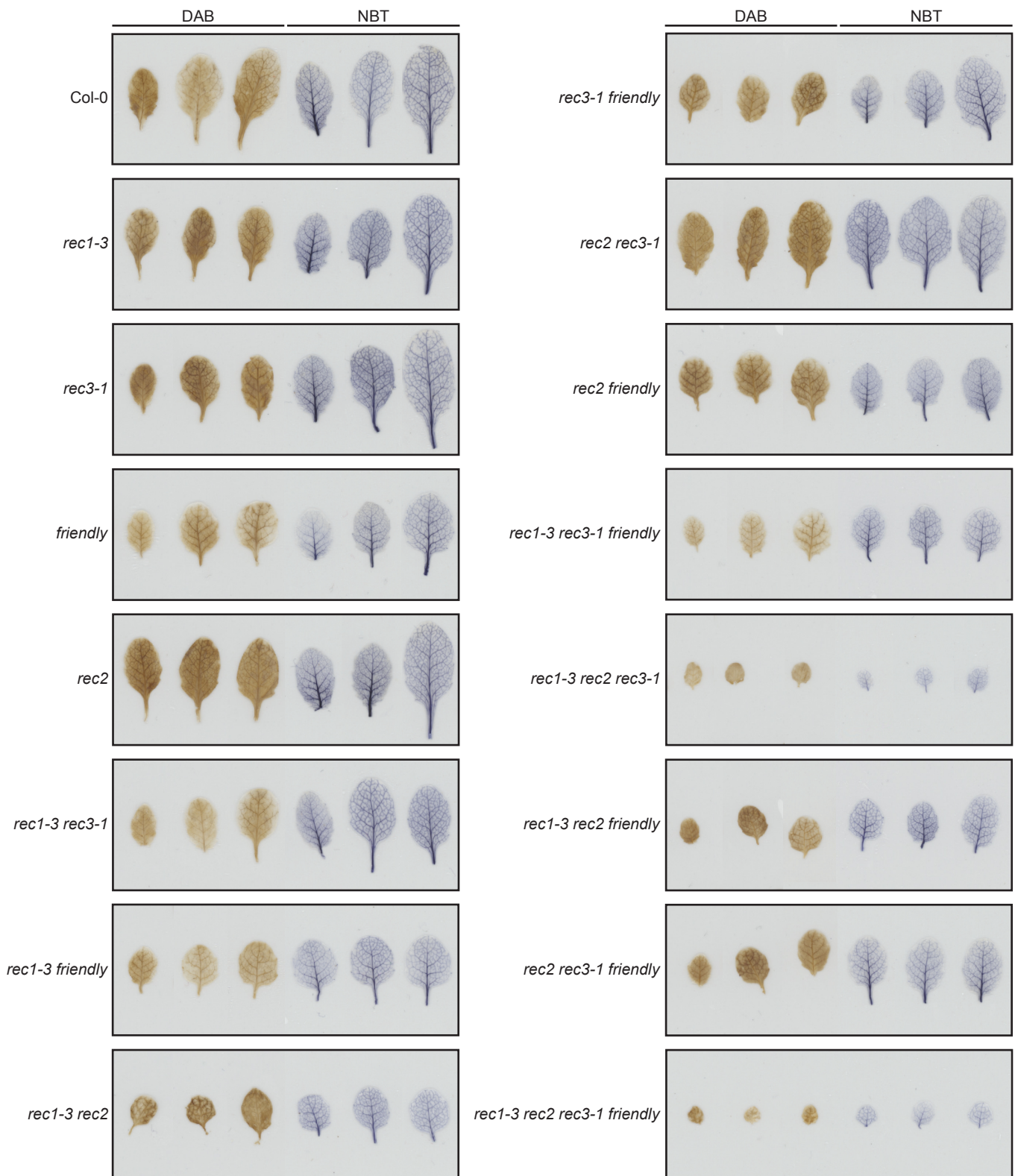


Fig. S16. DAB and NBT staining of leaves from the *REC* gene family mutants. The indicated lines were infiltrated with 3,3'-diaminobenzidine (DAB) and nitrotetrazolium blue (NBT) to detect hydrogen peroxide and superoxide, respectively. Representative leaves are shown.

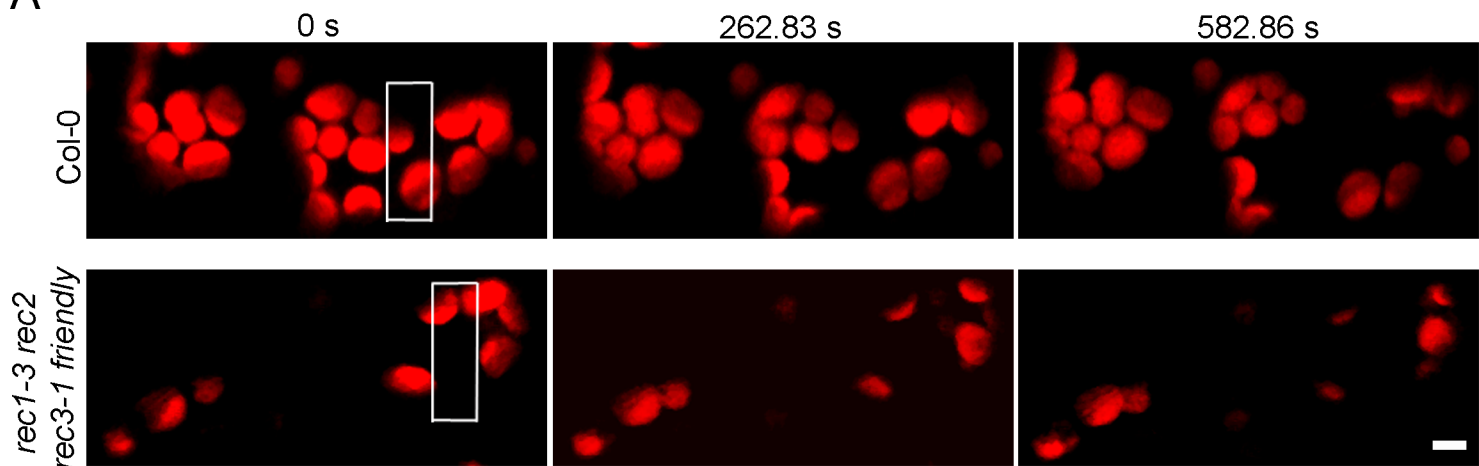
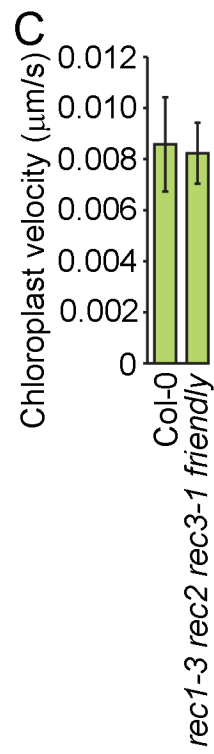
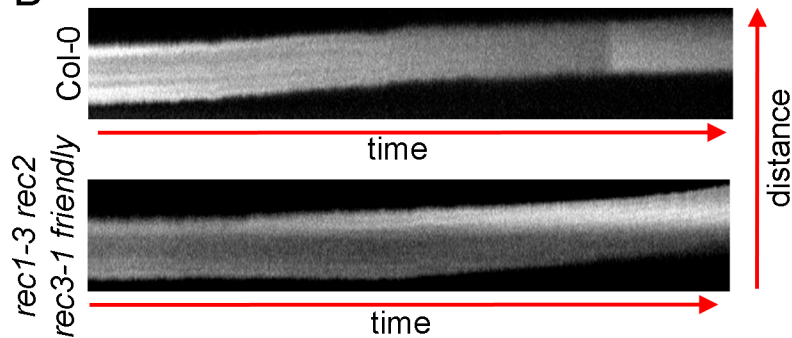
A**B**

Fig. S17. Comparison of chloroplast photorelocation in wild type and *rec1-3 rec2 rec3-1 friendly*.
(A) Photorelocation of chloroplasts in wild type and *rec1-3 rec2 rec3-1 friendly*.

Two cells are shown for wild type (Col-0) and *rec1-3 rec2 rec3-1 friendly*. The region of interest that was irradiated with a 488 nm laser at time zero is indicated with a white rectangle. The photorelocation of chloroplasts in the cells that were irradiated and the chloroplasts that did not photorelocate in the cells that were not irradiated are shown at 262.83 s and 582.86 s after the irradiation. Bar=10 μm .

(B) Representative kymographs.

Kymographs were derived from the maximum intensity projections of the trajectories generated by individual chloroplasts during photorelocation.

(C) Chloroplast velocity during photorelocation. The velocity of chloroplasts during relocation was calculated from kymographs based on the photorelocation of 26 different chloroplasts from 6 different cells of wild type and 39 chloroplasts from 6 different cells of *rec1-3 rec2 rec3-1 friendly*. Error bars represent 95% confidence intervals.

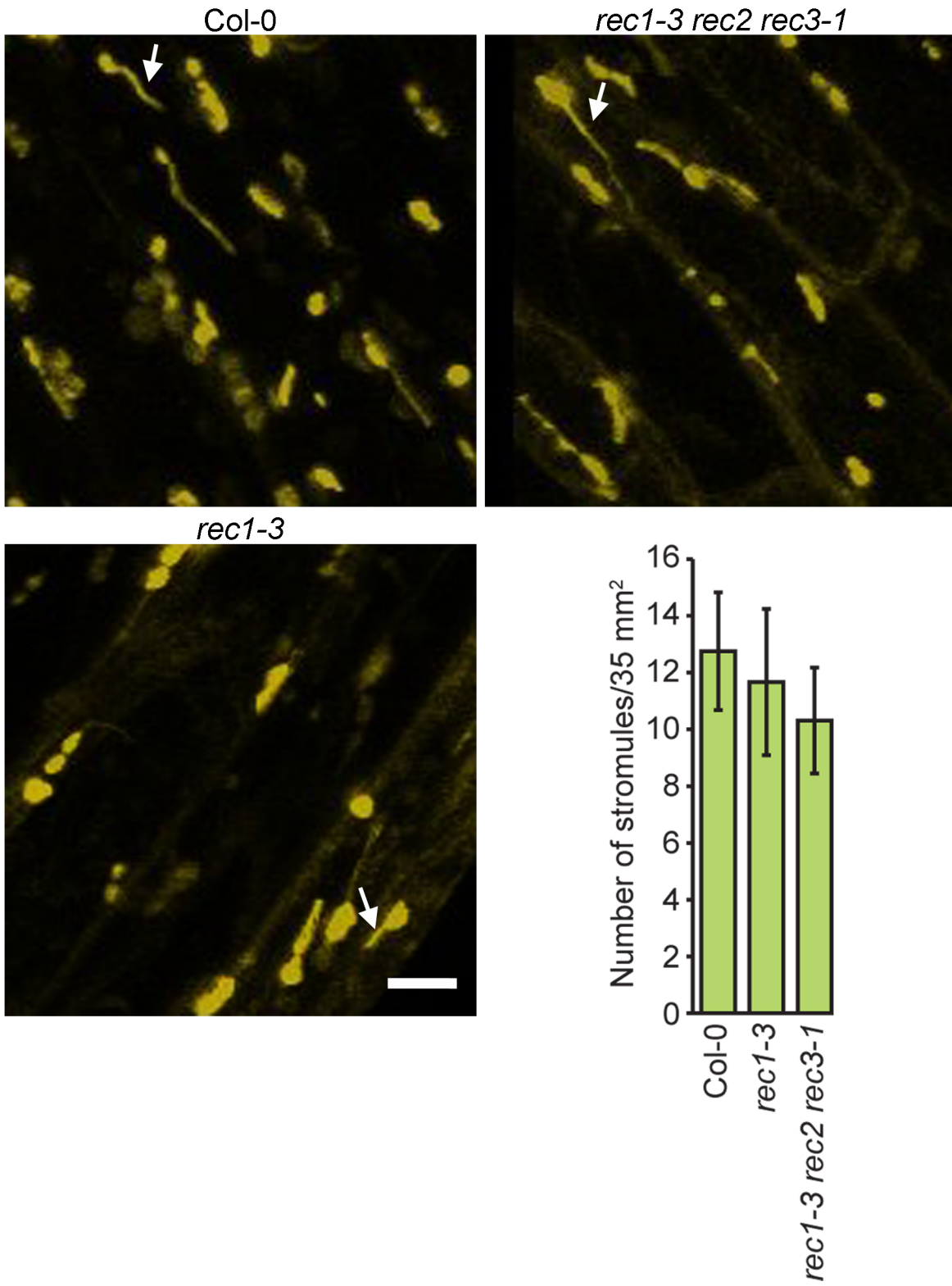


Fig. S18. Stromules in wild type, *rec1-3* and *rec1-3 rec2 rec3-1*.

Wild type (Col-0) and the indicated mutants were transformed with a transgene that targets YFP to the plastids. Seedlings were grown for 4 d in the dark to induce the elongation of the hypocotyls and then exposed to the light for 2.5 d to induce de-etiolation. The plastids of the hypocotyls were imaged with YFP fluorescence and confocal laser scanning microscopy. Bar=10 μ m. The number of stromules were counted in 13 to 16 micrographs derived from wild type and each mutant (lower right).

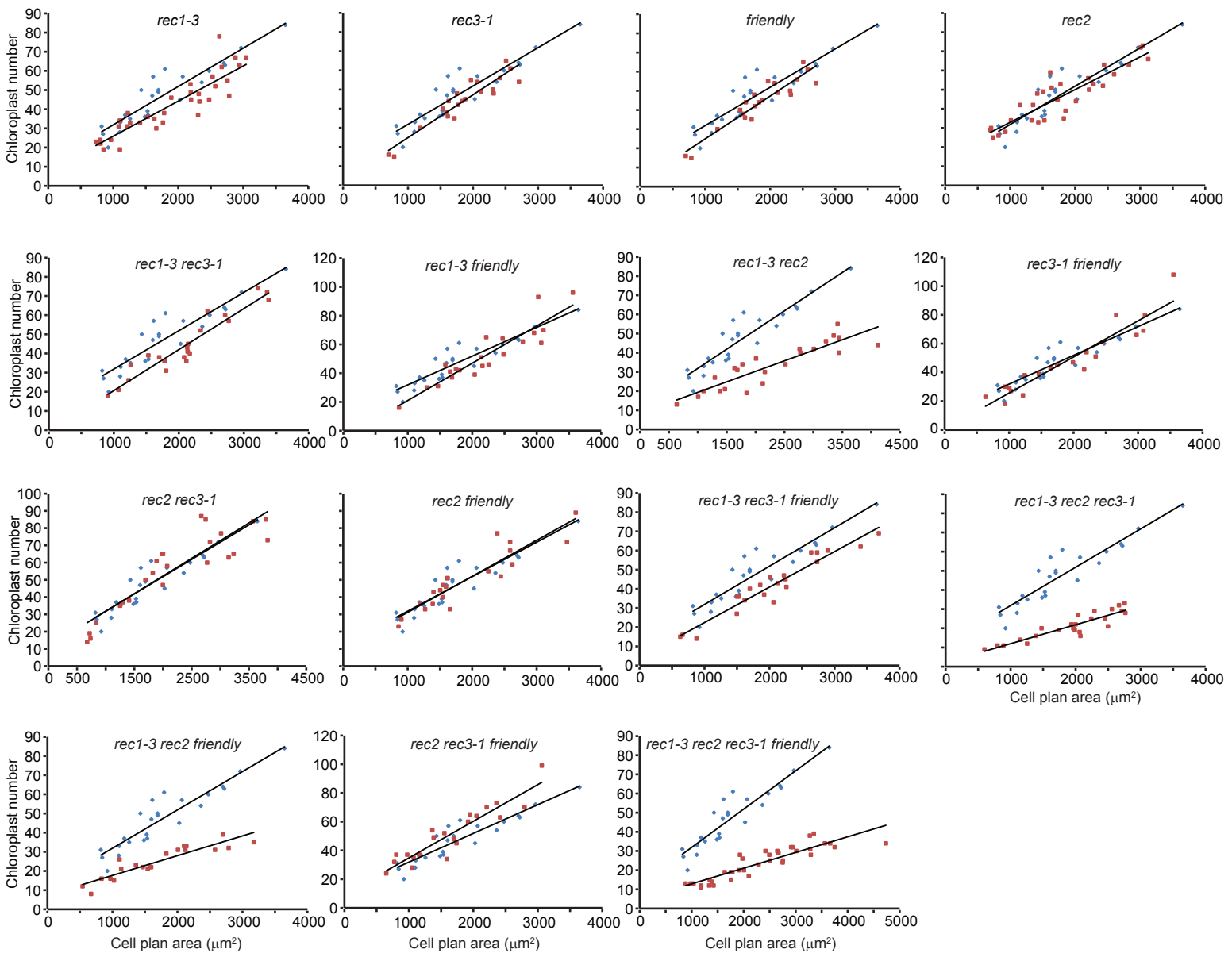


Fig. S19. Correlations between chloroplast number and cell plan area in the *REC* gene family mutants. Between 21 and 38 cells were analyzed from wild type and each mutant. Between 242 and 451 chloroplasts were analyzed from wild type and each mutant. Data from wild type is represented in each graph with blue diamonds. Data from the indicated mutant is represented with red squares. The number of chloroplasts was correlated with cell area in wild type and each mutant, $R^2=0.8$ to 0.95.

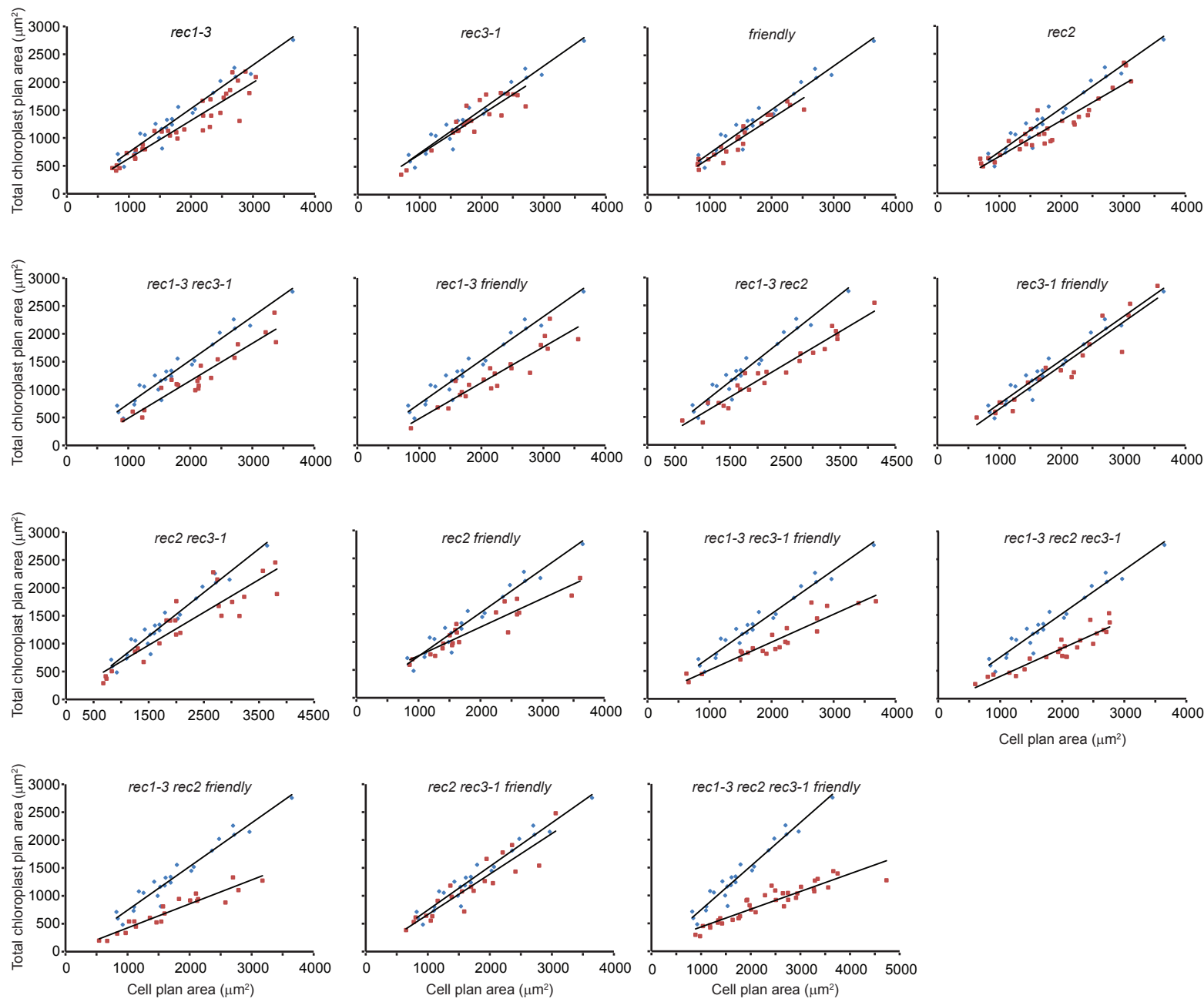


Fig. S20. Correlation between total chloroplast plan area and cell plan area in the *REC* gene family mutants. Between 21 and 38 cells were analyzed for wild type and each mutant. Between 242 and 451 chloroplasts were analyzed from wild type and each mutant. Data from wild type is represented in each graph with blue diamonds. Data from the indicated mutant is represented with red squares. The total chloroplast plan area was correlated with cell plan area in wild type and each mutant, $R^2=0.82$ to 0.95 .

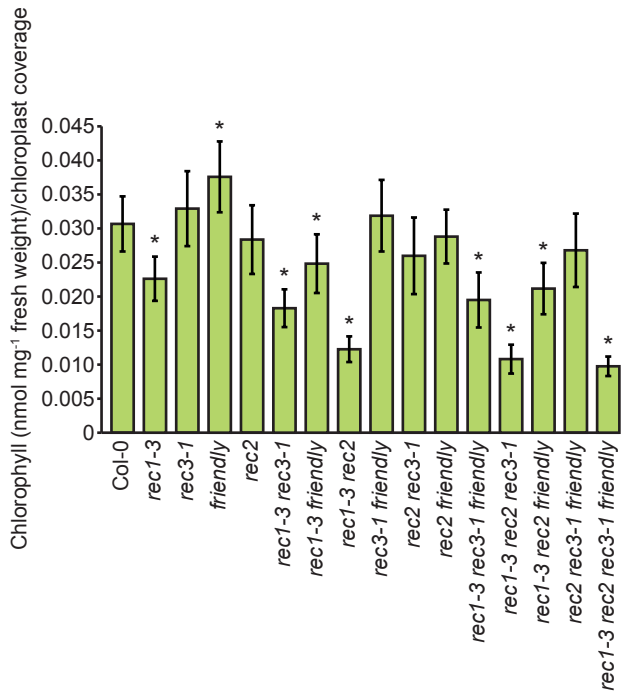


Fig. S21. Chlorophyll levels of the *REC* gene family mutants normalized to chloroplast coverage. Chlorophyll levels (Fig. 2) were normalized to chloroplast coverage (Fig. 4D) for wild type and each *REC* gene family mutant. Error bars indicate standard deviation. * indicates a statistically significant difference relative to wild type (Col-0) ($P < 0.0001$ to 0.04).

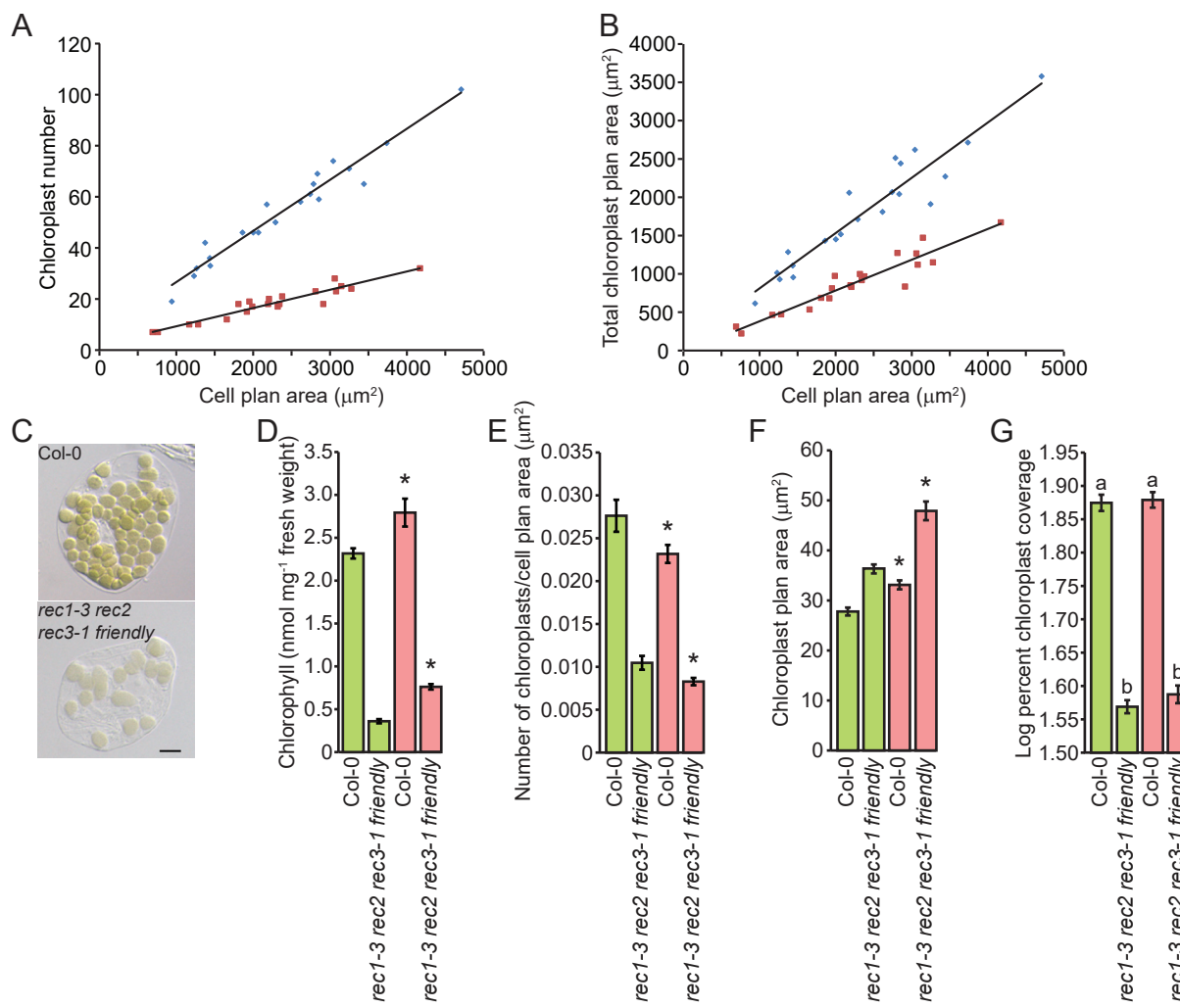


Fig. S22. Glutaraldehyde-fixed mesophyll cells from wild type and *rec1-3 rec2 rec3-1 friendly* grown in $35 \mu\text{mol m}^{-2} \text{s}^{-1}$ white light.

- (A) Correlations between chloroplast number and cell plan area in wild type and *rec1-3 rec2 rec3-1 friendly*. Plants were grown in soil for 30 d in $35 \mu\text{mol m}^{-2} \text{s}^{-1}$ white light. Twenty one cells were analyzed from wild type and *rec1-3 rec2 rec3-1 friendly*. A total of 343 and 196 chloroplasts were analyzed from wild type and *rec1-3 rec2 rec3-1 friendly*, respectively. Data from wild type is represented with blue diamonds. Data from *rec1-3 rec2 rec3-1 friendly* is represented with red squares. The number of chloroplasts was correlated with cell plan area in wild type and each mutant, $R^2=0.91$ and 0.95 .
- (B) Correlations between total chloroplast plan area and cell plan area in wild type and *rec1-3 rec2 rec3-1 friendly*. Plant growth, numbers of cells, numbers of chloroplasts and the representation of the data are as in (A), $R^2=0.90$.
- (C) Representative micrographs. Glutaraldehyde-fixed leaf mesophyll cells were visualized using differential interference contrast microscopy. Representative cells are shown. Bar=10 μm .
- (D) Chlorophyll phenotype. Plant growth was as in (A). Data from plants grown in $125 \mu\text{mol m}^{-2} \text{s}^{-1}$ white light is represented with green bars. Data from plants grown in $35 \mu\text{mol m}^{-2} \text{s}^{-1}$ white light is represented with red bars. Error bars indicate 95% confidence intervals. * indicates a statistically significant difference relative to the same line in $125 \mu\text{mol m}^{-2} \text{s}^{-1}$ white light ($P<0.0001$ and 0.0003).
- (E) Chloroplast number/cell plan area phenotype. Plant growth, bar color, error bars and * are as in (D) ($P=0.0003$ and 0.0004).
- (F) Plan area phenotypes of individual chloroplasts. Plant growth, bar color, error bars and * are as in (D) ($P<0.0001$).
- (G) Chloroplast coverage phenotype. A log transformation of the percent chloroplast coverage is presented. Plant growth and bar color are as in (D). Error bars represent SEM. Irradiance had no effect on log percent chloroplast coverage ($P = 0.338$). Values labeled with the same letter are not significantly different.

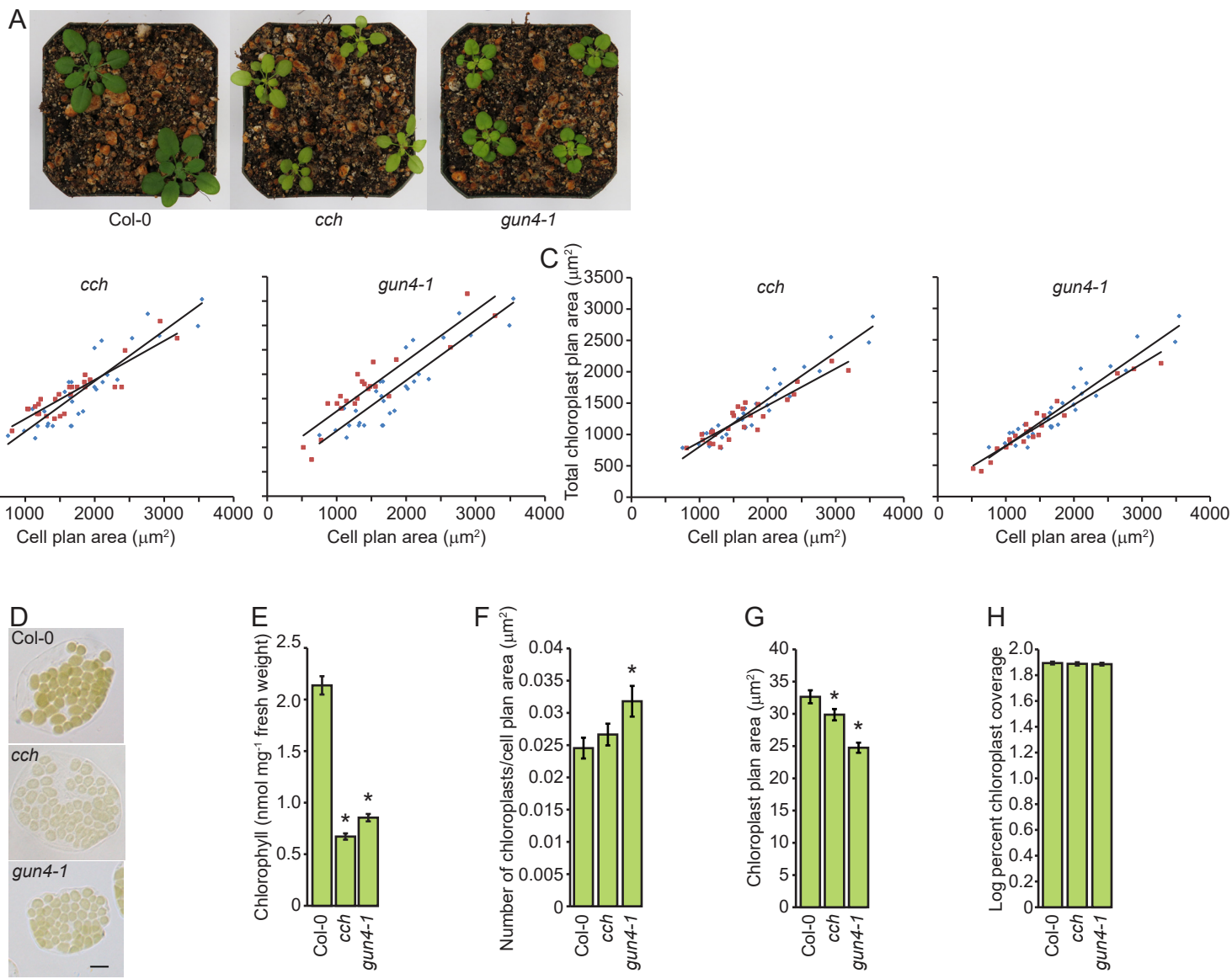


Fig. S23. Glutaraldehyde-fixed cells from wild type, *cch* and *gun4-1* in $35 \mu\text{mol m}^{-2} \text{s}^{-1}$ white light.
(A) Wild type (Col-0), *cch* and *gun4-1*. Plants were grown for 30 d in $35 \mu\text{mol m}^{-2} \text{s}^{-1}$ white light. Representative plants are shown.

(B) Correlations between chloroplast number and cell plan area in wild type, *cch* and *gun4-1*.

Plant growth was as in (A). Between 22 and 31 cells were analyzed from wild type, *cch* and *gun4-1*. Between 278 and 409 chloroplasts were analyzed from wild type, *cch* and *gun4-1*. Data from wild type is represented with blue diamonds. Data from the indicated mutant is indicated with red squares. The number of chloroplasts was correlated with cell plan area in wild type and each mutant, $R^2=0.80$ to 0.84 .

(C) Correlations between total chloroplast plan area and cell plan area in wild type, *cch* and *gun4-1*.

Plant growth was as in (A). Numbers of cells, numbers of chloroplasts and the representation of the data are as in (B). $R^2=0.84$ to 0.94 .

(D) Representative differential interference contrast micrographs.

Glutaraldehyde-fixed mesophyll cells were visualized using differential interference contrast microscopy.

Plant growth was as in (A). Representative cells are shown. Bar= $10\mu\text{m}$.

(E) Chlorophyll phenotypes. Plant growth was as in (A). Error bars indicate 95% confidence intervals.

* indicates a statistically significant difference relative to wild type (Col-0) ($P<0.0001$).

(F) Chloroplast number/cell plan area phenotypes. Plant growth, error bars and * are as in (E) ($P<0.0001$).

(G) Plan area phenotypes of individual chloroplasts. Plant growth, error bars and * are as in (E) ($P<0.0001$).

(H) Chloroplast coverage. A log transformation of the percent chloroplast coverage is presented. Error bars represent SEM. Plant growth was as in (E). Genotype had no effect on log percent chloroplast coverage ($P = 0.857$).

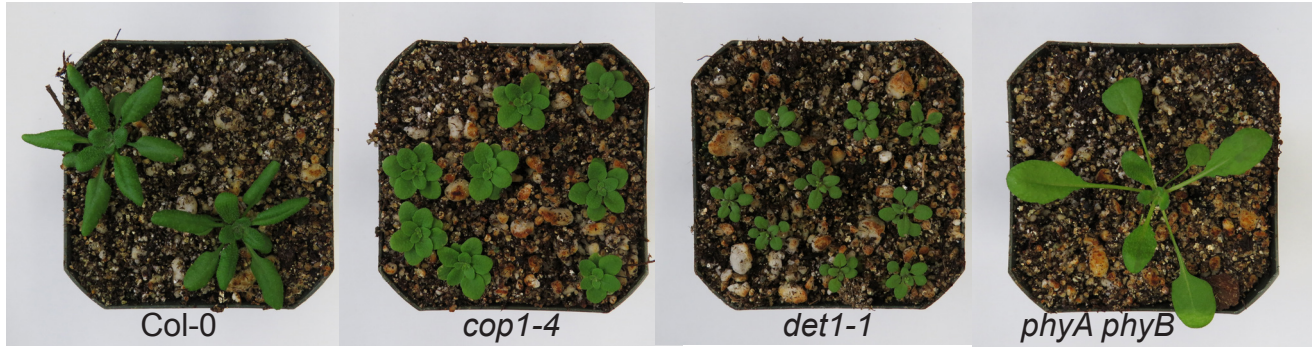


Fig. S24. Wild type (Col-0), *cop1-4*, *det1-1* and *phyA phyB*. Representative 24-d-old plants are shown.

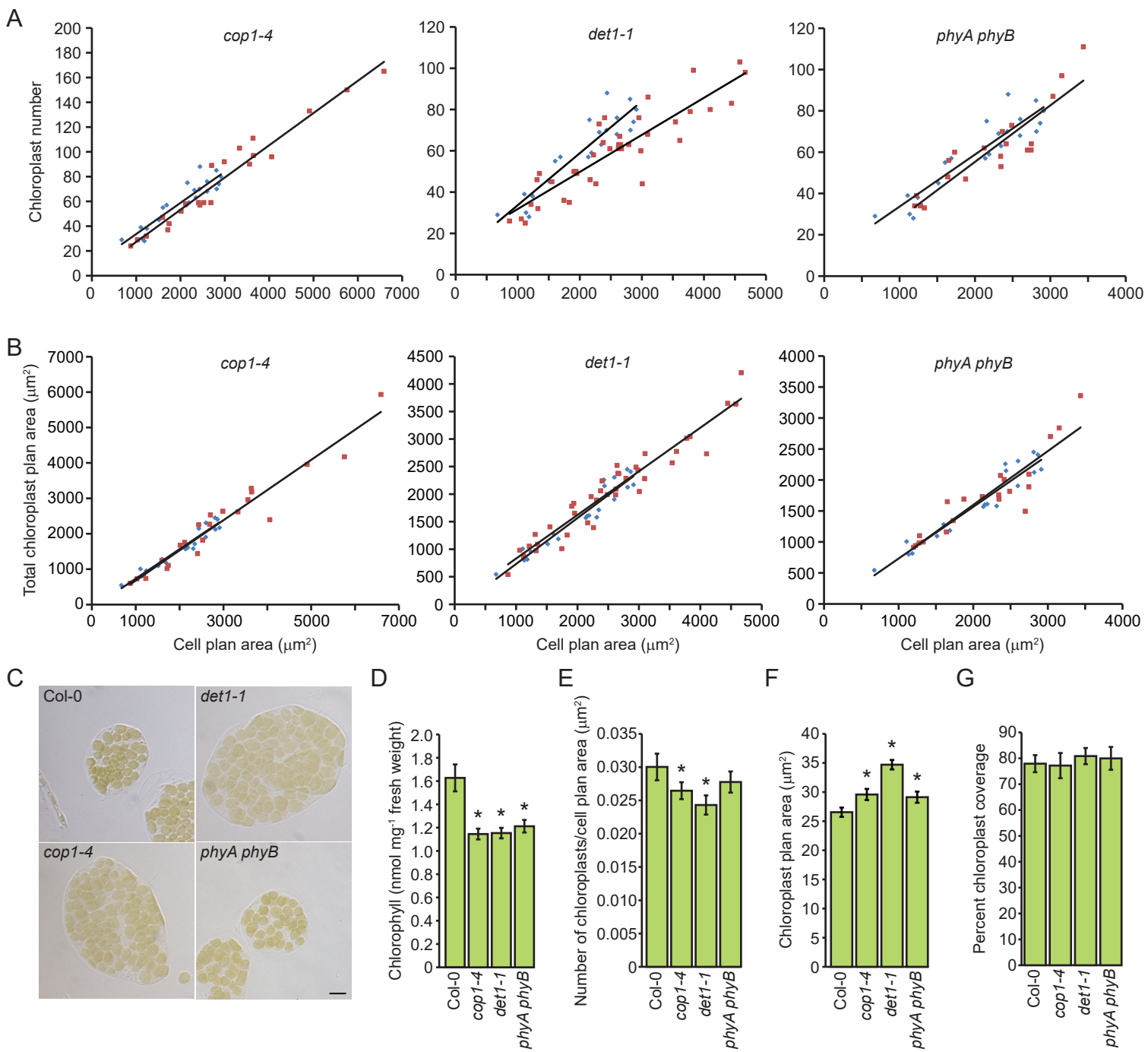


Fig. S25. Glutaraldehyde-fixed mesophyll cells from wild type, *cop1-4*, *det1-1* and *phyA phyB*.

(A) Correlations between chloroplast number and cell plan area in wild type, *cop1-4*, *det1-1* and *phyA phyB*. Between 21 and 39 cells were analyzed from wild type, *cop1-4*, *det1-1* and *phyA phyB*. Between 289 and 536 chloroplasts were analyzed from wild type, *cop1-4*, *det1-1* and *phyA phyB*. Data from wild type is represented with blue diamonds. Data from each mutant is indicated with red squares. The number of chloroplasts were correlated with cell plan area in wild type and in each mutant, $R^2=0.79$ to 0.95.

(B) Correlations between total chloroplast plan area and cell plan area in wild type, *cop1-4*, *det1-1* and *phyA phyB*. Number of cells, number of chloroplasts and presentation of the data are as in (B). Total chloroplast plan area was correlated with cell plan area in wild type and each mutant, $R^2=0.84$ to 0.93.

(C) Glutaraldehyde-fixed cells. Representative cells are shown. Bar=10 μm .

(D) Chlorophyll levels in wild type, *cop1-4*, *det1-1* and *phyA phyB*. Error bars indicate 95% confidence intervals.

* indicates a statistically significant difference relative to wild type ($P<0.0001$).

(E) Chloroplast number/cell plan area phenotypes of wild type, *cop1-4*, *det1-1* and *phyA phyB*. Error bars and * are as in (D) ($P<0.0001$ to 0.005).

(F) Plan area phenotypes of individual chloroplasts from wild type, *cop1-4*, *det1-1* and *phyA phyB*. Error bars and * are as in (D) ($P<0.0001$).

(G) Chloroplast coverage phenotypes in wild type, *cop1-4*, *det1-1* and *phyA phyB*. Error bars are as in (D).

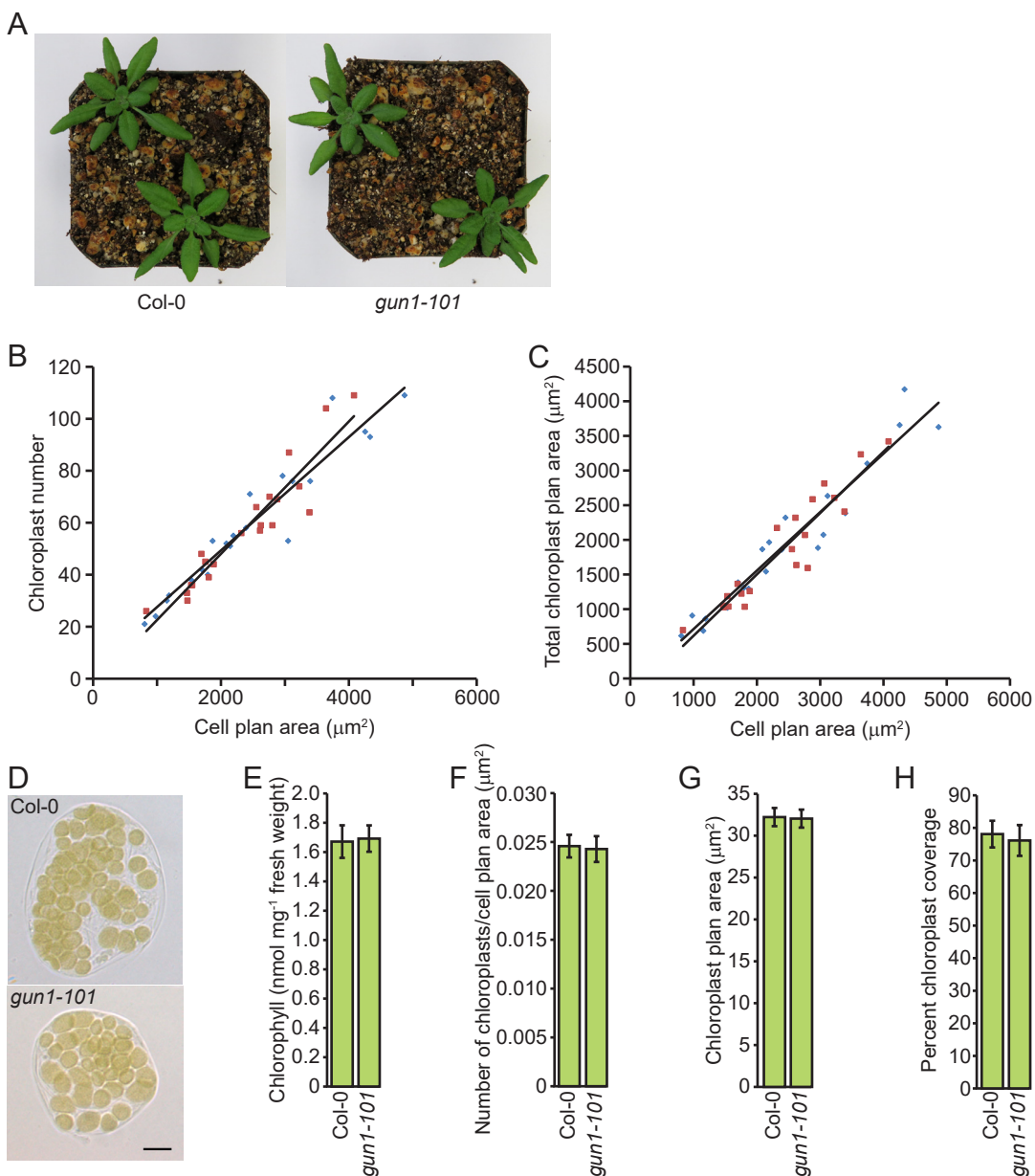


Fig. S26. Characterization of wild type and *gun1-101*.

(A) Wild type and *gun1-101*. Representative 24-d-old plants are shown for wild type (Col-0) and *gun1-101*.

(B) Correlations between chloroplast number and cell plan area in wild type and *gun1-101*. Twenty one cells were analyzed from wild type and *gun1-101*. A total of 299 and 277 chloroplasts were analyzed from wild type and *gun1-101*, respectively. Data from wild type is represented with blue diamonds. Data from *gun1-101* is indicated with red squares. The number of chloroplasts were correlated with cell plan area in wild type and *gun1-101*, $R^2=0.89$ and 0.92.

(C) Correlations between total chloroplast plan area and cell plan area in wild type and *gun1-101*. The number of cells, number of chloroplasts and presentation of the data are as in (B). Total chloroplast plan area was correlated with cell plan area in wild type and each mutant, $R^2=0.88$ and 0.93.

(D) Glutaraldehyde-fixed cells. Representative cells are shown. Bar=10 μm .

(E) Chlorophyll levels in wild type and *gun1-101*. Error bars indicate 95% confidence intervals.

(F) Chloroplast number/cell plan area phenotypes of wild type and *gun1-101*. Error bars are as in (E).

(G) Plan area phenotypes of individual chloroplasts from wild type and *gun1-101*. Error bars are as in (E).

(H) Chloroplast coverage phenotypes in wild type and *gun1-101*. Error bars are as in (E).

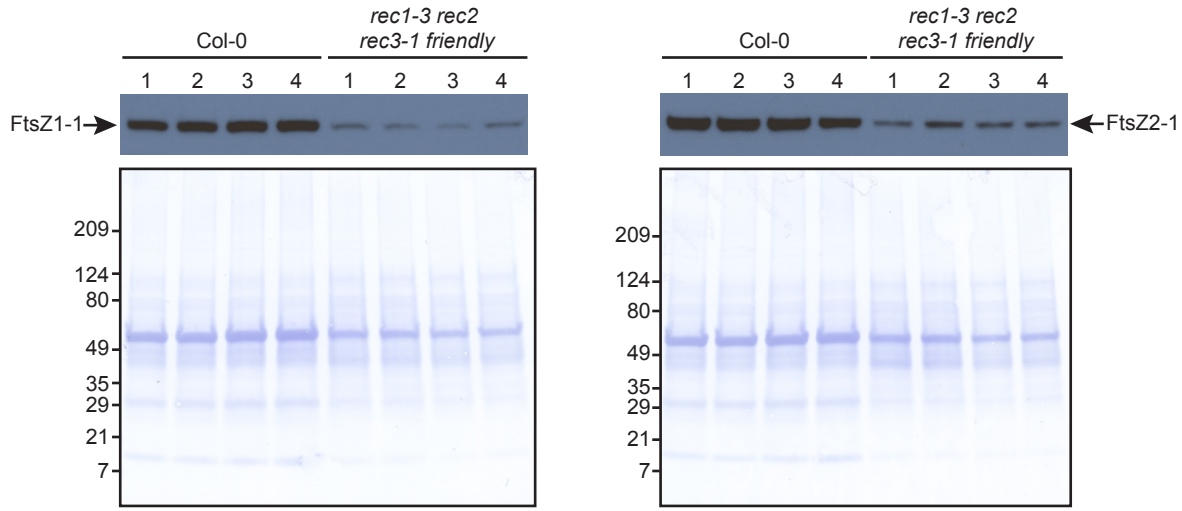


Fig. S27. FtsZ1-1 and FtsZ2-1 in wild type and *rec1-3 rec2 rec3-1 friendly*.

Whole seedling extracts were prepared from 8-d-old wild type (*Col-0*) and *rec1-3 rec2 rec3-1 friendly* that were grown on LS medium containing 1% sucrose. Ten µg of protein was analyzed from four biological replicates using SDS-PAGE and immunoblotting with anti-FtsZ1-1 and FtsZ2-1 antibodies (above). The immunoreactive bands composed of FtsZ1-1 and FtsZ2-1 are indicated with arrows. After immunoblotting, the polyvinylidene fluoride membranes were stained with Coomassie brilliant blue R-250 (below). The mass of each protein standard is indicated at the left in kDa.

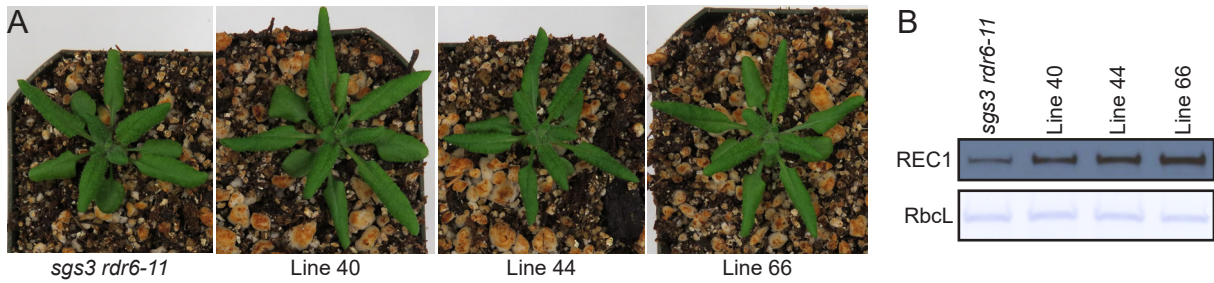


Fig. S28. Overexpression of *REC1* in *sgs3 rdr6-11*.

(A) *sgs3 rdr6-11* and transgenic plants 40, 44 and 66 that overexpressed *REC1*.

(B) Immunoblotting of whole-leaf extracts from *sgs3 rdr6-11* and *sgs3 rdr6-11* that overexpressed *REC1*. Whole leaf extracts were prepared from 24-d-old plants. Extracts were analyzed by immunoblotting with affinity purified anti-*REC1* antibodies (above). After immunoblotting, the polyvinylidene fluoride membrane was stained with Coomassie blue R-250. The predominant Coomassie blue-stained band composed of the large subunit of RuBisCO (RbcL) is shown (below). Each lane contains 3 µg of protein.

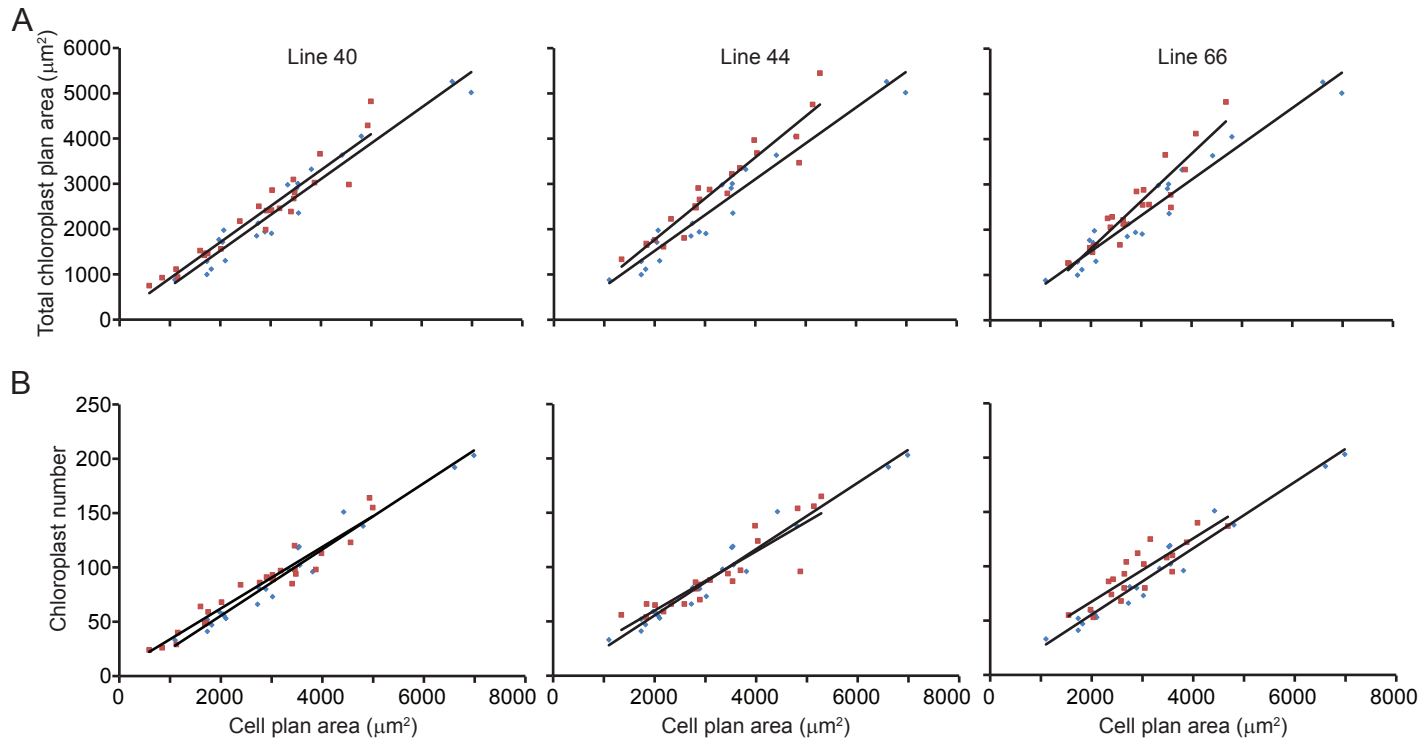


Fig. S29. Analysis of mesophyll cells from *sgs3 rdr6-11* that overexpressed *REC1*.

(A) Correlations between total chloroplast plan area and cell plan area in *sgs3 rdr6-11* and transgenic plants that overexpressed *REC1*. Between 21 and 25 cells were analyzed from *sgs3 rdr6-11* and transgenic lines 40, 44 and 66 that overexpressed *REC1*. Between 430 and 482 chloroplasts were analyzed from *sgs3 rdr6-11* and the transgenic plants. Data from *sgs3 rdr6-11* is represented with blue diamonds. Data from each transgenic plant is represented with red squares. Total chloroplast plan area was correlated with cell plan area in *sgs3 rdr6-11* and each transgenic plant, $R^2=0.88$ to 0.94.

(B) Correlations between chloroplast number and cell plan area in *sgs3 rdr6-11* and transgenic plants that overexpressed *REC1*. The number of cells and chloroplasts analyzed was as in (A). The data from *sgs3 rdr6-11* and each transgenic plant are represented with blue diamonds and red squares as in (A). The number of chloroplasts was correlated with cell plan area in *sgs3-rdr6-11* and each transgenic plant, $R^2=0.79$ to 0.96.

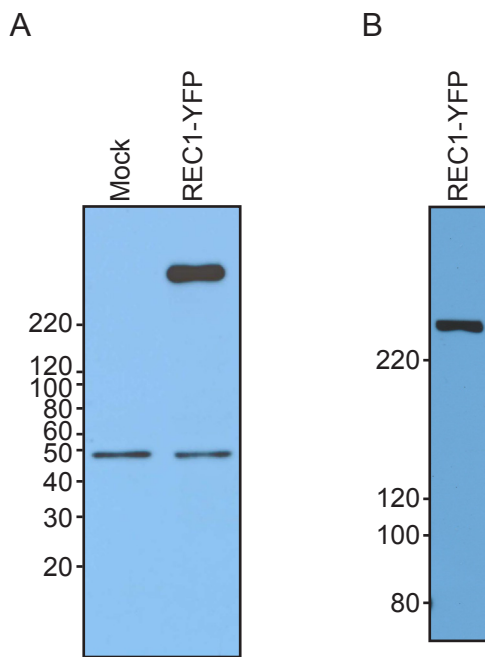


Fig. S30. Immunoblotting of whole-leaf extracts from tobacco cells transiently expressing REC1-YFP.
 (A) Transient transfection with REC1-YFP. Whole-leaf extracts were prepared from equal amounts of leaves using denaturing conditions after a transient transfection with an *Agrobacterium* strain harboring the REC1-YFP transgene (REC1-YFP) or a mock transfection with the same *Agrobacterium* strain lacking the REC1-YFP transgene (Mock). Equal volumes from the REC1-YFP-transfected leaves and the mock-transfected leaves were analyzed by SDS-PAGE with a 4 to 20% gradient gel and immunoblotting using anti-GFP antibodies. The intensities of the background band of approximately 50 kDa indicate that similar amounts of protein were loaded in each lane. The mass of each standard protein is indicated at the left in kDa.
 (B) Estimation of the mass of REC1-YFP. The whole-leaf extract described in (A) was analyzed by SDS-PAGE with a 5% gel and immunoblotting as described in (A). The mass of each standard protein is indicated at the left in kDa.

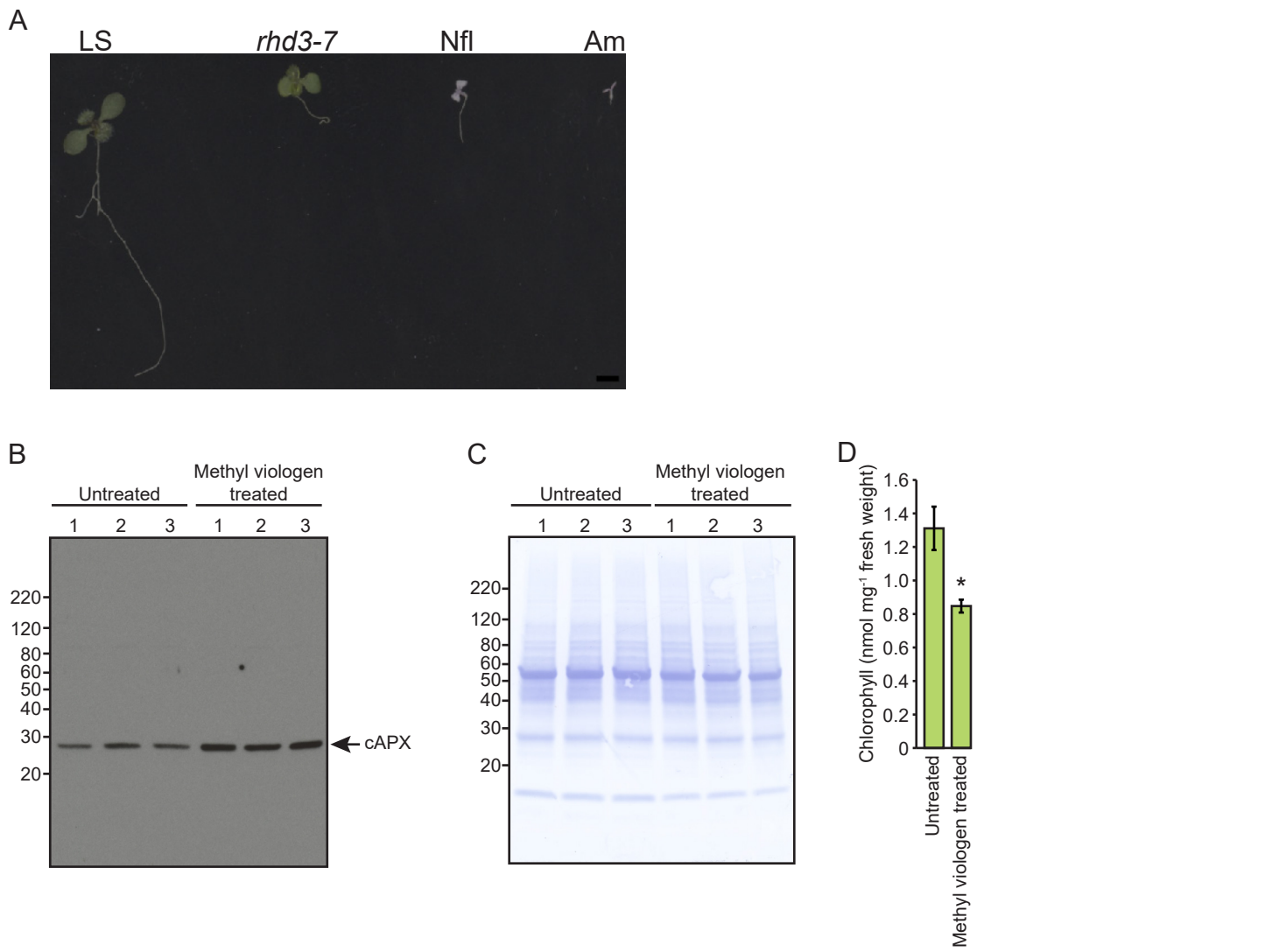


Fig. S31. Herbicide-treated seedlings.

(A) Untreated and herbicide treated seedlings.

Wild type seedlings were grown for 8 d on media containing no herbicide (LS), norflurazon (Nfl) or amitrole (Am). *rhd3-7* was grown on a medium containing no herbicide. Bar=2mm.

(B) Cytosolic ascorbate peroxidase levels in methyl viologen-treated and untreated seedlings.

Whole-seedling extracts were prepared from three biological replicates of methyl viologen-treated or untreated 8-d-old seedlings using denaturing conditions. Ten µg of protein was analyzed using SDS-PAGE and immunoblotting with anti-cytosolic ascorbate peroxidase antibodies. The immunoreactive band composed of cytosolic ascorbate oxidase (cAPX) is indicated with an arrow. The mass of each standard protein is indicated at the left in kDa.

(C) Total protein analysis of the immunoblot from (B).

After immunoblotting, the polyvinylidene fluoride membrane was stained with Coomassie brilliant blue R-250. The mass of each protein standard is indicated at the left in kDa.

(D) Chlorophyll levels in methyl viologen-treated and untreated seedlings.

Five biological replicates were analyzed for methyl viologen-treated and untreated seedlings. Error bars indicate 95% confidence intervals. * indicates a statistically significant difference relative to untreated ($P=0.0001$).

Table S1. Oligonucleotides used for identifying T-DNA insertions in *REC1* and related genes

	1	2	3	4
<i>REC1</i>	At1g01320	SAIL_555_D11	CCACTGCTGTTCCATTG/	
		Salk_049453	CATGTGTATCATCTTTGTCGTAG/	
		Salk_132306	GCAGCTACGACTGGTCCATG/	
<i>REC2</i>	At4g28080	Salk_020337	GCAGCAGTATCAGCCTCTGAAGA/	
		Salk_131245	GATCCTGTCCGTTGATATGC/	
<i>REC3</i>	At1g15290	SAIL_633_B04	CTTACGGTTATGTGCAGTTCTC/	
		SAIL_1164_H02	CTTCGTATAAGTTGCTCCTGG/	
			GAAGTTGGTGTTCAGCTTG/	
<i>FMT</i>	At3g52140	Salk_056717	TCAGCTCCAAGTAGTCTCTGG/	
			TAAAGGCAAACGGAGGATGC/	
			CGAACCTTGCACACAGGTAC/	
			CATCAACCACGAGTGCCATG/	
			AGAGTAGTATCGAGACCAACA/	
			GAACAGGAGAAGGTACAAGC/	
			GCGAAAGTTGCATTATGAATGG/	
			CTCGTGTCTAGAATCATCG	

1. Gene name, 2. AGI number, 3. Salk or SAIL line, 4. Oligonucleotide sequences (right primer /left primer).

Table S2. Oligonucleotides used for RT-PCR analysis of *REC1* and related genes

	1	2	3	4
<i>REC1</i>	At1g01320	Exon 4 and exon 6 Exon 11 and exon 12 Exon 24	GTATCCTTCGACGCAGGAG/ GGACAGGATCATAGATGTTGG TGAGCATTCTCTCAGCATCG/ CTTGAACAGCCTGAAGGTGG CGTTCACTGCGTGCAACTG/ GACTCTCATCACGGACCTC	
<i>REC2</i>	At4g28080	Exon 5 and exon 8 Exon 23	TCTCCTACCTTACTCCTCCG/ GCTTCATAAGAGCGTCATAAGC GGTGCAGAAATAAACACAGAATGG/ TGCTCGATTTCATTATCGCTG	
<i>REC3</i>	At1g15290	Exon 2 and exon 4 Exon 11 and exon 13 Exon 20 and exon 21	CTGGTTGAAATCACAGTCACC/ GCTACAATGTCGATGACTCTCC ACTCCAATGCGTTCTCTAGG/ CAGAGCTCATGAAAGGATTGG GTTGCTCACAGGAAACATCG/ GTTGACTCTCCACAGTTGC	
<i>FMT</i>	At3g52140	Exon 2 and exon 4 Exon 26 and exon 28	TCACTGCTGTTGACTCTGC/ TGAAGTAGCACGTCTCTGG AGACGTTAACATGCGTGAGC/ CTTCTCAGACGAAACTGTGG	

1. Gene name, 2. AGI number, 3. Exons that contain oligonucleotide binding sites, 4. Sequences of forward/reverse oligonucleotides

Table S3. Markers used for fine-mapping *rec1-1*

1	2	3	4
T25K16	TCTTCAGCCTAAAACAGTCTCC/ CGGAAATAATCAAATCGGAAGC	N/A	(143)/(152)
F6F3-90	TTTCTCGACTGTTCATAGAGC/ TGTCTGACAGATCTGATGAG	Hinf I	(225)/117 + 108
F6F3-97	GATATTGGTGTAGAAGCGACG/ AAAACCAACATGAGGATTCTAACTG	Bbs I	105 + 114/(219)
F6F3-105	GGTAGATCCTCGATTCTTCAGG/ AAAGAAACCAGCTCATCGACC	Hae II	150 + 77/(227)
F6F3-117	GAGAACAGTCTCACTCGC/ GGAGTCACGTTGGAGACG	BamH I	235 + 112/ 217 + 130
F22L4	ATTGGTTTACTGGATTGCTCCC/ TCTTGCCCTGGTGTCCAAG	N/A	(163)/(155)
T1N6	CAGTCGTAATCTGATGACGTTC/ CTGCAAGGTGTTCACATCTG	Ase I	152 + 149/(301)

1. Marker name. 2. Oligonucleotide primer sequences (RP/LP). 3. Restriction endonucleases. 4. Lengths of (undigested) and digested PCR products from Col-0/*Ler* in base pairs. The names of the PCR-based markers incorporate the names of the bacterial artificial chromosome clones from which they were derived. PCR-based markers are listed from the most centromere distal (T25K16) to the most centromere proximal (T1N6).

SI Materials and Methods

Plant materials and growth conditions

All mutants used in this study were derived from *Arabidopsis thaliana* ecotype Columbia-0 (Col-0). The Col-0 line harboring the *Lhcb:luc+* reporter gene and the EMS mutagenesis of this line was described in Ruckle et al. (1). T-DNA insertion mutants (2, 3) and *rdr6-11* were obtained from the Arabidopsis Resource Center (Columbus, OH). We analyzed three publicly available T-DNA insertion alleles of *REC1*: *rec1-2* (SAIL_555_D11), *rec1-3* (Salk_049453) and *rec1-4* (Salk_132306). We analyzed publicly available T-DNA insertion alleles for *REC2*, *REC3* and *FRIENDLY*. We refer to these alleles as *rec2* (Salk_020337), *rec3-1* (SAIL_633_B04), *rec3-2* (SAIL_1164_H02) and *friendly* (Salk_056717). *rec1-3*, *rec2*, *rec3-1* and *friendly* were used for the construction of double, triple and quadruple mutants. Single, double, triple and quadruple mutants were identified among the progeny that resulted from crosses using PCR-based markers (Table S1). *rec1-1* was identified using a cleaved amplified polymorphic sequence (CAPS) marker (4) that utilized 5'-GCTCATCCCTTGTAAGCTCC-3', 5'-AAGTGAAGCCTACCACACG-3' and the restriction endonuclease Mse I. We characterized *rec1*, *rec2*, *rec3* and *friendly* mutants by comparing the levels of mRNA transcribed from each T-DNA allele to the levels of mRNA transcribed from the corresponding wild-type gene using RT-PCR and gene-specific oligonucleotides (Table S2) as described by Ruckle et al. (1). The double mutant used for *REC1* overexpression experiments was constructed by crossing *sgs3* (5) and *rdr6-11* (6).

Plants were grown in controlled-environment chambers in either white light or far-red light. When grown in soil, unless indicated otherwise, plants were grown at 20°C in 125 $\mu\text{mol m}^{-2} \text{s}^{-1}$ white light provided by broad-spectrum fluorescent tube lamps with a photoperiod of 16 h of light followed by 8 h of dark. To grow plants on soil, seeds were stratified for 4 d at 4°C in 0.1% Phytoblend (Caisson Laboratories, Inc., Logan UT). Seeds were then dispersed on top of sterile soil that was a 1:1:1 mixture of Baccto High Porosity Professional Planting Mix (Michigan Peat Company, Houston TX): vermiculite: perlite in controlled-environment chambers. To grow plants on a growth medium, seeds were surface sterilized by washing them with a tube mixer in 70% ethanol containing 0.5% Triton X-100 for 5 min, followed by 95% ethanol for 5 min and then dried on filter paper (Whatman International Ltd., Maidstone UK) that was soaked in 95% ethanol in a laminar-flow hood. Surface-sterilized seeds were dispersed on Linsmaier and Skoog (LS) medium (Caisson Laboratories) that contained 0.5% Phytoblend. After stratification for 4 d at 4°C, seedlings were grown in continuous white light at an irradiance of 80 $\mu\text{mol m}^{-2} \text{s}^{-1}$ at 21°C, unless indicated otherwise. To test for *gun* phenotypes, seedlings were grown on LS medium that also

contained 2% sucrose and either 5 μ M norflurazon (Sigma-Aldrich, St. Louis MO) or 0.5 mM lincomycin (Sigma-Aldrich).

The experiments that tested for a far-red block of greening phenotype were adapted from previously published work (7). The far-red light was provided by light-emitting diodes. The far-red light peak was at 739 nm with a spectral bandwidth of 31 nm. Far-red light was passed through one filter (number 116, Lee Filters, Andover UK) to remove wavelengths that were less than 700 nm. For far-red light, irradiance was measured with a StellarNet EPP2000 spectroradiometer (Apogee Instruments, Logan UT). All other irradiance measurements were performed with an LI-250A photometer using a PAR sensor (LI-COR Biosciences, Lincoln NE). For far-red block of greening experiments, seeds were surface sterilized and plated on LS growth medium without sucrose. After plating, seeds were stratified for at least 4 d at 4°C, irradiated with 125 μ mol m⁻² s⁻¹ red light for 1 h, germinated in the dark for 36 h, grown in 2 μ mol m⁻² s⁻¹ far-red light for 2.5 d, transferred to 60 μ mol m⁻² s⁻¹ white light for 4.5 d and then scored for cotyledons that were green or not green (i.e., white or pale yellow). The statistical significance of the differences between the proportions of seedlings that greened in the different genotypes was determined by tests of the equality of two proportions, as implemented in Systat 13.1 (Systat Software, Inc., San Jose, CA, USA). For this test, we pooled the number of seedlings of each status (green or not green) for each line from replicate experiments, in which values were similar. For each mutant line, we then tested the hypothesis that the proportions of seedlings that were either green or not green in the mutant lines and in wild type were equal.

Sequence alignments and phylogenetic analysis

Amino acid sequences were obtained from the National Center for Biotechnology Information based on their similarity to the REC1 amino acid sequence. The amino acid sequence alignment was prepared with MEGA5 using MUSCLE and edited using BioEdit (8). Motifs were identified using PROSITE (9). Phylogenetic analysis was performed at www.phylogeny.fr (10, 11).

Map-based cloning of *rec1-1*

rec1-1 was isolated by first mutagenizing a Col-0 line that harbored the *Lhcb:luc+* reporter gene and then by screening for the upregulation of *Lhcb:luc+* and endogenous PhANGs in norflurazon- and lincomycin-treated seedlings (i.e., the *gun* phenotype) as described in Ruckle et al. (1). The *rec1-1* allele was rough mapped by crossing *rec1-1* with a Landsberg *erecta* (*Ler*) line, in which the *Lhcb:luc+* transgene was introgressed from the Col-0 *Lhcb:luc+* line by seven crosses to *Ler*. We mapped *rec1-1* to 700 kb at the top of chromosome 1 by scoring the *gun* phenotype and by analyzing 230 chromosomes

from the F2 progeny yielded by this cross. A smaller interval was not obtained because both the *gun* phenotype and the far-red block of greening phenotype were not possible to unambiguously score in these F2 progeny. We overcame this problem by crossing *rec1-1* to the recombinant inbred lines (RILs) CL67, CL35 and CL115 (12). These RILs were derived from Col-4 and *Ler*. Their chromosomes are largely composed of DNA from Col-4. However, the first 20 to 60 cM of chromosome 1 is enriched in DNA from *Ler*. The attenuation of the far-red block of greening phenotype in the F2 progeny yielded from the cross between *rec1-1* and these RILs was not as severe as in the F2 progeny yielded from the cross between *rec1-1* and *Ler Lhcb:luc+*. To fine map the far-red block of greening phenotype of *rec1-1*, we analyzed 2376 chromosomes from the F2 progeny yielded by the cross between *rec1-1* and the RILs using PCR-based markers (4, 13, 14) that were designed using the Cereon Arabidopsis Polymorphism Collection (15) (Table S3). The far-red block of greening phenotype was confirmed in the F3 progeny for all F2 plants that were used for the fine mapping of *rec1-1*.

Fine mapping yielded a 70-kb interval. To sequence genes in this 70-kb interval, genes were first amplified by means of GoTaq Flexi DNA Polymerase (Promega, Madison WI) in at least 10 independent aliquots using gene-specific oligonucleotides. These aliquots were subsequently pooled. PCR products were purified by electrophoresis in agarose gels and by extracting PCR products from agarose gels using the QIAquick gel extraction kit (Qiagen, Valencia CA). Purified PCR products were sequenced with gene-specific oligonucleotides by the Michigan State University (MSU) Research Technology Support Facility

Development and purification of anti-REC1 antibodies

A fragment of the *REC1* gene that encodes residues P1419 to F1673 was cloned into pHIS8-3 (16). This *REC1* fragment was expressed as a His-tagged protein in *E. coli* strain BL21-Codon Plus (DE3)-RIPL (Stratagene, Santa Clara CA) according to the manufacturer's recommendations. When whole-cell extracts were analyzed by SDS PAGE and Coomassie brilliant blue R-250 staining, this fragment accumulated to barely detectable levels. Unless indicated otherwise, the following steps were performed at 4°C. Bacteria that expressed the His-tagged fragment of REC1 were resuspended in buffer A (50 mM Tris HCl, pH 7.9, 500mM NaCl, 20mM imidazole, 20mM β-mercaptoethanol, 20% glycerol) that also contained 4 mM Pefabloc SC (Roche, Indianapolis IN). The bacteria were resuspended in 20 mL of buffer A per gram of bacteria. While stirring, 1mg/mL lysozyme and then 1.0% Triton X-100 were added to the resuspended bacteria. The viscosity of the resulting solution was reduced with an ultrasonic processor (Cole Parmer, Vernon Hills IL). The homogenate was clarified by centrifugation at 20,000 × g. The His-tagged proteins in the clarified supernatants were batch-bound to Ni-NTA agarose (Qiagen) that

was equilibrated in buffer A. The Ni-NTA agarose was batch-washed twice with buffer A containing 1.0% Triton X-100 and then batch-washed twice with buffer A. The washed Ni-NTA-agarose was poured into an Econo-Pac column (Bio-Rad, Hercules CA). Proteins were step-eluted using buffer B (20 mM Tris HCl, pH 7.9, 500 mM NaCl, 250 mM imidazole, 20 mM β -mercaptoethanol, 20% glycerol). Eluted proteins were dialyzed against buffer C (20mM Tris-HCl pH 7.9, 150 mM NaCl, 2.5 mM CaCl₂, 20mM β -mercaptoethanol, 20% glycerol), digested with thrombin (Sigma-Aldrich) at room temperature to remove the His tag, dialyzed against buffer D (20 mM Tris-HCl, pH 7.9, 100 mM NaCl, 1 mM EDTA, 1 mM DTT, 20% glycerol), and then applied to a Mono Q HR10/10 column (GE Healthcare, Piscataway NJ) that was equilibrated in buffer D. Proteins were eluted from the column with a 160-mL linear gradient to buffer E (20 mM Tris-HCl, pH 7.9, 500 mM NaCl, 1 mM EDTA, 1 mM DTT, 20% glycerol) at 1mL/min. The 4-mL fractions were pooled if they contained bands whose mobility increased following the aforementioned thrombin digestion. The pooled fractions were concentrated with an Amicon Ultra Centrifugal Filter (Millipore Corporation, Billerica MA) and then applied to a HiLoad 26/60 Superdex 200 column (GE Healthcare, Piscataway NJ) that was equilibrated in buffer F (20 mM Tris-HCl, pH 7.9, 500 mM NaCl, 1 mM EDTA, 1 mM DTT, 10% glycerol) at 2 mL/min. The 8-mL fractions were pooled if they contained bands whose mobility increased following the aforementioned thrombin digestion. The pooled fractions were concentrated with an Amicon Ultra Centrifugal Filter (Millipore Corporation), dialyzed extensively against phosphate buffered saline and used to develop polyclonal antisera in New Zealand White rabbits at Strategic Diagnostics, Inc. (Newark DE).

The affinity purification of the anti-REC1 antibodies was performed essentially as described previously for anti-Mg-chelatase subunit antibodies (17). The only modification was that the affinity purification of the anti-REC1 antibodies was performed with a resin that was constructed by linking the purified REC1 fragments described above to AffiGel 15 (Bio-Rad).

Preparation and analysis of whole-leaf extracts

Leaves from 24-d-old plants grown in soil were frozen with liquid N₂. The frozen leaf tissue was powdered with a TissueLyser (Qiagen) that was set at the maximum frequency (30 Hz) for 30 sec. The frozen powder was suspended in SDS-PAGE sample buffer (18) and immediately incubated in a boiling water bath for 5 min. After cooling to room temperature, the samples were clarified at 16,000 \times g for 10 min at 25°C. The protein concentrations of the supernatants (i.e., the whole-leaf extracts) were determined using the Pierce 660 nm protein assay reagent (Thermo Scientific, Waltham MA).

Quantitation of mRNA levels

Quantitative analysis of *Lhcb1.2* and *RbcSA1* expression by qRT-PCR was performed as described previously (5) with modifications. RNA was extracted from 7-d-old seedlings as described previously (1). Relative mRNA levels were calculated using the comparative C_T method (19). Relative mRNA levels were expressed relative to the levels of mRNA derived from *UBQ10*. Error bars represent a range calculated with the equation $2^{-\Delta\Delta CT \pm \text{standard deviation}}$ as recommended by Applied Biosystems (Foster City, CA). P values were calculated from mean $\Delta\Delta CT$ values and the standard error of the mean derived from these $\Delta\Delta CT$ values using an unpaired t test. Four biological replicates were analyzed for each line in each condition.

Quantitation of chlorophyll and protochlorophyllide levels

To quantify the levels of chlorophyll, two leaves of intermediate age were collected for each biological replicate (e.g., 15 to 30 mg of leaves from plants grown in soil). Unless indicated otherwise, leaves were collected from 24-d-old plants that were grown in soil. Leaves were flash frozen in liquid N₂ and stored at -80°C. Chlorophyll was extracted using N, N'-dimethylformamide and quantified as described previously (20) except that biological replicates were homogenized in 1.7 mL microfuge tubes that contained a single 3 mm very high density zirconium oxide bead (Glen Mills Inc., Clifton NJ) using a TissueLyser (Qiagen) that was set at the maximum frequency (30 Hz) for 5 min.

To quantify the levels of protochlorophyllide that accumulated in far-red light, seeds were surface sterilized, plated on LS medium, stratified for at least 4 d at 4°C and exposed to 150 $\mu\text{mol m}^{-2} \text{s}^{-1}$ white light for 1 h. Seedlings were grown for 23 h in the dark and then grown for 3 d in 2 $\mu\text{mol m}^{-2} \text{s}^{-1}$ far-red light. Protochlorophyllide was extracted from seedlings and quantified essentially as recommended by Rebeiz (21). Briefly, seedlings were homogenized in acetone: 0.1 N NH₄OH (9:1) using a TissueLyser, as described for chlorophyll extractions. Protochlorophyllide was subsequently separated from esterified tetrapyrroles with three hexane extractions. The relative levels of protochlorophyllide in the resulting extracts were determined by quantifying protochlorophyllide fluorescence in a black-walled 96-well plate with a clear bottom (Corning Inc., Corning NY) in a SpectraMax M2 microplate reader (Molecular Devices, Sunnyvale CA) as recommended by Rebeiz (21).

Quantitation of hypocotyl lengths in far-red light

To quantify hypocotyl lengths, seeds from wild type (Col-0), *rec1-3* and *rec1-3 rec2 rec3-1 friendly* were surface sterilized, plated on ½ strength LS growth medium without sucrose and stratified as described in the plant materials and growth conditions section above. Germination was induced with red light as described for the far-red block of greening experiments. Seedlings were grown in either 3 $\mu\text{mol m}^{-2} \text{s}^{-1}$

far-red light or in the dark for 4 d. Seedlings were imaged between acetate sheets with a flatbed scanner. Hypocotyl lengths were quantified using Fiji (22) as recommended by Fankhauser and Casal (23). Four biological replicates were analyzed for wild type and each mutant in each condition. Each biological replicate was composed of at least 10 seedlings.

Transmission electron microscopy

Plants were grown in soil for 22 d. Sections were obtained from the terminal ca. 25% of leaves. Leaf sections were fixed in 0.1 M cacodylate, pH 7.4, 2.5% glutaraldehyde, 2.5 % paraformaldehyde at 4°C for 24 hours, postfixed in 1% osmium tetroxide in 0.1M cacodylate, pH 7.4, and dehydrated in a graded acetone series. Samples were infiltrated and embedded in Poly/Bed 812 Embedding Media (Polysciences, Warrington PA). Sections of 70 nm were prepared using a PT-XL PowerTome Ultramicrotome (Boeckeler Instruments, Tucson AZ) on 200 mesh copper grids stained with uranyl acetate and lead citrate. Sections were imaged using a JEOL 100CX II transmission electron microscope with an accelerating voltage of 100kV.

Analysis of chloroplasts using confocal laser scanning microscopy

An inverted Zeiss LSM510 META confocal laser scanning microscope equipped with an EC Plan-Neofluar 40x/1.30 objective (<http://www.zeiss.com/>) was used for confocal laser scanning microscopy. Chlorophyll was excited using a 514 nm argon laser. Chlorophyll fluorescence was collected from 650 to 700 nm (24, 25). Confocal images were acquired always using the same fixed laser intensity, pinhole, gain and zoom. For each Z stack, between 25 and 40 sections of 1 μm were collected from the abaxial surface of the leaf beginning in the epidermis and ending in the cortical region of the spongy mesophyll. Five to seven images were collected for each mutant. Maximum intensity projections were calculated from each Z stack. The fluorescence values were calculated and plotted using Image Pro-Plus 6 (Media Cybernetics). The fractal dimensions and lacunarity parameters (26) were calculated from the maximum intensity projections using fraclac, an ImageJ plugin (27). The statistical significance of the differences between these values in the different mutants relative to the values in wild type was calculated with an unpaired t test.

To test whether the *rec* and *friendly* alleles affect the photorelocation of chloroplasts, wild type and *rec1-3 rec2 rec3-1 friendly* were grown in 35 $\mu\text{mol m}^{-2} \text{s}^{-1}$ white light in soil for 26 d. Chloroplast movement was analyzed with the same microscope that was used to image chlorophyll fluorescence. Chloroplast photorelocation was performed by repeatedly irradiating the region of interest for 2.02 sec with a 488 nm laser at 3% of maximum power throughout the photorelocation experiment. Chlorophyll fluorescence was

imaged between irradiations of the region of interest. During the photorelocation experiment, chlorophyll was excited using a 633 nm laser and fluorescence was collected from 650 to 700 nm (24, 25). For each movie, the fluorescence of chloroplasts located in the cortical region of the spongy mesophyll was acquired.

To calculate chloroplast velocities, maximum intensity projections of individual chloroplasts were generated from a time lapse series to define the trajectory of individual chloroplasts. Kymographs were generated from these trajectories. The velocities of individual chloroplasts were calculated from the kymograph lines using the Multi Kymograph plugin for ImageJ 1.49n essentially as described by Deng et al. (28) and Tan et al. (29). The velocities calculated for the chloroplasts from wild type and *rec1-3 rec2 rec3-1 friendly* were based on 26 and 39 kymographs, respectively, from 6 independent cells.

Detection of reactive oxygen species

Hydrogen peroxide and superoxide were detected by staining with 3, 3'-diaminobenzidine (DAB) and nitrotetrazolium blue (NBT), respectively. Plants were grown in soil for 23 d or 25 d and then fed with DAB or NBT, respectively, by immersing the roots in either 25 mM DAB or 6 mM NBT for 4 h in the dark, as recommended by Woo et al. (30). After feeding with DAB or NBT, plants were returned to the growth chamber for 1 h. Chlorophyll was removed from the leaves by immersing the leaves in ethanol, lactic acid and glycerol (4:1:1) and incubating the leaves at 80°C for 25 min, as recommended by Driever et al. (31). The leaves were immersed in fresh ethanol, lactic acid and glycerol solution overnight to remove residual chlorophyll from the leaves. After the chlorophyll was extracted, leaves were arranged and imaged between acetate sheets as recommended by Woo et al.(30) and Driever et al. (31).

Differential interference contrast microscopy

The terminal ca. 25% of rosette leaves that were of an intermediate age from 22-d-old plants grown in soil were removed with a razor blade. Leaf sections were fixed with glutaraldehyde as described previously (32, 33). Fixed mesophyll cells were released from the leaf sections as described previously (32, 33). The fixed chloroplasts and mesophyll cells were visualized using differential interference contrast microscopy with a Leica DMI3000B inverted microscope. The micrographs were collected with a Leica DFC320 camera. The plan areas of chloroplasts and leaf mesophyll cells were quantified using Fiji (22). Three different biological replicates were analyzed for wild type and each mutant. At least seven cells were analyzed from each biological replicate. For overexpression experiments, single transgenic plants were analyzed because of the variability in the overexpression of REC1. From 242 to 535 chloroplasts from 21 to 39 cells were analyzed for wild type and each mutant. The number of chloroplasts/cell plan area,

chloroplast plan areas and total chloroplast plan area/cell plan area (i.e., chloroplast coverage) were calculated as described previously (32, 33).

For the number of chloroplasts/cell plan area and chloroplast plan areas, the statistical significance of the differences between the different genotypes was evaluated with an unpaired t test. In evaluating the percent chloroplast coverage data, we recognized that percent data may not exhibit normal distributions if fixed numerical boundaries (0%-100%) constrain the shape of the distributions. However, we found that the percent chloroplast coverage metric used here does not typically suffer from these bounding problems because chloroplasts are essential organelles (chloroplast numbers do not reach zero) and because percent chloroplast coverage is a two-dimensional metric used to describe the three-dimensional cellular structure (so maximum values can exceed 100%). Thus, in our data sets, minimum values did not fall below 29% and maximum values approached 130%. Each percent chloroplast coverage data set was then evaluated for normality and homoscedasticity and was log-transformed as needed or for the sake of consistency with other data sets when such a transformation was valid. Untransformed and log-transformed data were evaluated in Systat 13.1 with Levene's Test for Homogeneity of Variances and the Anderson-Darling Test for Normality. The statistical significance of differences among genotypes was tested using a one-way categorical analysis of variance (ANOVA) and a posthoc Dunnett Test (two-sided). For the *REC* gene family mutants, we also conducted a two-way categorical ANOVA that considered the interacting effects of *rec1-3* (presence/absence) and the number of mutant alleles (1, 2 or 3) on chloroplast coverage. This analysis was conducted on the log-transformed data from 14 lines representing the relevant factor values, omitting wild type and the quadruple mutant.

Overexpression of *REC1*

To overexpress *REC1*, the *REC1* gene containing part of the 5' untranslated region, the complete coding sequence and the complete 3' untranslated region was amplified from the bacterial artificial chromosome clone F6F (Arabidopsis Resource Center) using *PfuUltra* II Fusion HS DNA Polymerase (Agilent Technologies, Santa Clara CA) and the oligonucleotides 5'-
GAGATTATTGCAATTAACCAAGTTGAATTG-3' and 5'-
CTACCTGCCAATTAGAGATCAACAAAG-3'. This PCR product was inserted downstream of the 35S promoter in pGWB2 (34). The 5' -untranslated region of the mRNA derived from this transgene is composed of sequence from *REC1* and pGWB2 with a length of nearly 160 bases. After finding that no mutations were introduced into *REC1* by sequencing *REC1* at the MSU Research Technology Support Facility, this transgene was introduced into *sgs3 rdr6-11* double mutant (6) using the floral dip method (35). Transformants were selected on ½ strength LS medium containing 30 µg/mL hygromycin and 100

μ g/mL ampicillin. Hygromycin-resistant seedlings were transferred to soil. The relative levels of REC1 in the leaves of these primary transformants were determined by analyzing whole-leaf extracts prepared as described above using immunoblotting (36) with the affinity-purified anti-REC1 antibodies described above. Briefly, gels were electroblotted in 25 mM Tris, 192 mM glycine and 0.025% SDS. Immunoreactive bands were identified using SuperSignal West Dura Extended Duration Substrate (Thermo Fisher Scientific Inc., Waltham, MA). Plants that accumulated elevated levels of the REC1 protein relative to *sgs3-rdr6-11* were propagated. In the next generation, the numbers of chloroplasts/cell plan area, the plan areas of individual chloroplasts and chloroplast coverage in leaf mesophyll cells from glutaraldehyde-fixed leaf sections were determined in transgenic plants that accumulated elevated levels of the REC1 protein.

Construction and expression of YFP fusion genes

To visualize the subcellular distribution of REC1, the open reading frame (ORF) that encodes the yellow fluorescent protein (YFP) was fused in frame and downstream of the full-length ORF that encodes REC1. A cDNA clone that contains the full-length *REC1* ORF was obtained by extracting total RNA from 7-d-old *Arabidopsis* seedlings using the RNeasy Plant Mini Kit (Qiagen). cDNA was synthesized from total RNA using oligo(dT)₁₂₋₁₈ primers (Invitrogen, Carlsbad CA) and Superscript II reverse transcriptase (Invitrogen). cDNAs that contain the full-length *REC1* ORF were amplified from this cDNA using gene-specific oligonucleotides 5'-GACGTCTAGATGGCTCCCAAGAACAAAC-3', 5'-CATGACCCTCGAGATACTACAGACTTGGAGC-3' and Phusion High-Fidelity DNA polymerase (New England BioLabs, Ipswich MA). The full-length cDNA was cloned into pCR 8/GW/TOPO (Invitrogen) using the pCR 8/GW/TOPO TA cloning kit (Invitrogen). Next, the full-length *REC1* ORF was fused to the enhanced yellow variant of GFP (YFP) and cloned into pVKh18-EN6 (37). To accomplish this cloning, the *REC1*- pCR 8/GW/TOPO plasmid was digested with XbaI and Xho I. pVKh18-EN6 was digested with Xba I and Sal I. Restriction fragments were purified using agarose gel electrophoresis and the DNA Clean & Concentrator-5 Kit (Zymo Research, Irvine CA). Purified restriction fragments were ligated with T4 DNA ligase (New England Biolabs). Plasmids were propagated in *E. coli* strain DH5 α and sequenced to test for mutations at the MSU Research Technology Support Facility.

Transient expression of REC1-YFP in *Nicotiana tabacum* was performed by infiltrating leaves with *Agrobacterium tumefaciens* GV3101 strains that harbored the REC1-YFP fusion gene in pVKh18-EN6 as described previously (37). Tobacco plants were grown in controlled-environment chambers with white light provided by broad-spectrum fluorescent tube lamps and incandescent bulbs at 75 μ mol m⁻² s⁻¹. Days

were 16 h and 23°C. Nights were 8 h and 18°C. The live-cell confocal microscopy analyses of YFP fluorescence (37) and the immunoblotting analysis of the YFP-fusion protein were performed 2 d after infiltration. Whole-leaf extracts were prepared using denaturing conditions as described above. Supernatants were analyzed by SDS-PAGE and immunoblotting with anti-GFP antibodies (Abcam, Cambridge UK) as described above for anti-REC1 antibodies except that the SDS gels were electroblotted in 25 mM Tris, 192 mM glycine and 10% methanol.

To test whether the functional state of the chloroplast affected the subcellular distribution of the REC1-YFP, REC1-YFP was transiently expressed in leaves that were made chlorophyll deficient with an amitrole treatment. Amitrole inhibits the accumulation of chlorophyll (38). To treat tobacco leaves with amitrole, single leaves of tobacco plants were infiltrated with 125 µM amitrole (Sigma-Aldrich) in H₂O. Leaves did not appear chlorophyll deficient at the site of infiltration, but leaves that developed from the shoot apical meristem following this infiltration appeared chlorophyll deficient. These observations are consistent with amitrole moving from the site of infiltration to the shoot apical meristem and inhibiting the chloroplast biogenesis that occurs during leaf development from the shoot apical meristem. Transient expression was performed in chlorophyll-deficient leaves that developed 7 to 10 d after infiltrating with amitrole.

To detect stromules, a transgene that targets YFP to chloroplasts was constructed. In this transgene, the DNA sequence encoding the transit peptide from the *Arabidopsis RbcS1A* gene was fused downstream of the 35S promoter from cauliflower mosaic virus and also fused in frame and upstream of YFP in pVKh18-EN6 (37). The sequence encoding the transit peptide from *RbcS1A* was amplified from the publicly available cDNA clone U13397 that was obtained from the *Arabidopsis* Biological Resource Center (Columbus, Ohio). PCR utilized *PfuTurbo* DNA polymerase (Agilent, Santa Clara CA) and the oligonucleotides 5'-ACATTTACATTCTACAACATATGGCTTCCTATGC-3' and 5'-GCCCTTGCTCACCATCATGCAGTTAACTCTTCC-3'. This PCR product was inserted into pVKh18-EN6 (37) that was linearized with Sal I and Xba I using the Gibson Assembly Master Mix (New England BioLabs, Ipswich MA). The resulting transgene was sequenced at the MSU Research Technology Support Facility. Wild type and the indicated mutants were transformed with this transgene using the floral dip method (35). Transgenic plants were selected on ½ strength LS medium containing 30 µg/mL hygromycin and 100 µg/mL ampicillin. Seeds were collected from plants exhibiting YFP fluorescence. To image the plastids and stromules, seeds from plants that exhibited YFP fluorescence were germinated on LS medium containing 1% sucrose by exposing the seedlings to 150 µmol m⁻² s⁻¹ white light for 2.5 h. Seedlings were grown in the dark for 4 d and then transferred to the light for 2.5 d. The stromules were

imaged in the hypocotyls of these seedlings using confocal laser scanning microscopy. Four to five images were collected from four different transgenic plants for wild type and each mutant. The number of stromules was counted in each micrograph. The statistical significance of the differences in the number of stromules in the different mutants and wild type was calculated with an unpaired t test.

Collecting images of YFP fluorescence using confocal laser scanning microscopy

Fluorescence imaging was performed using either a Zeiss 510 Meta ConfoCor3 Confocal Laser Scanning Microscope (Carl Zeiss MicroImaging, Thornwood NY) or an Olympus Fluoview 1000 Confocal Laser Scanning Microscope (Olympus America Inc., Center Valley PA) at the MSU Center for Advanced Microscopy. For the Zeiss microscope, a 514-nm line from an argon laser was used to excite YFP. A 633-nm line from a helium-neon laser was used to excite chlorophyll. Emission from YFP and chlorophyll was filtered with 530 to 600 nm and 647 to 754 nm filters, respectively, using appropriate main dichroics. Samples were viewed with a 63 \times oil-immersion objective. Zeiss AIM software and Paint Shop Pro (Corel, Ottawa Canada) were used for postacquisition image handling. For the Olympus microscope, a 514-nm line from an argon laser was used to excite YFP. A 635-nm line from a solid-state laser was used to excite chlorophyll. Emissions from YFP and chlorophyll were filtered with 515 to 575 nm and 655 to 755 nm filters, respectively, using appropriate main dichroics. Samples were viewed with a 60 \times oil-immersion objective. The Olympus Fluoview Viewer software Ver.02.1b was used for postacquisition image handling. For each experiment 50-100 cells were examined in one plant. Each experiment was repeated 3-5 times. Different plants were used for each repetition. Representative images are presented.

Preparation and analysis of whole-seedling extracts, nuclear fractions and cytosolic fractions

For whole-seedling extracts that were compared to nuclear extracts and cytosolic fractions, seedlings grown on the same plates as seedlings that were used for the purification of nuclei and cytosolic fractions were frozen with liquid N₂ and used to prepare whole-seedling extracts as described for whole-leaf extracts. For the purification of nuclei, 8-d-old seedlings were grown on LS medium without sucrose or LS medium containing 1% sucrose and either 5 μ M norflurazon or 100 μ M amitrole. To facilitate harvesting, seedlings were grown on sterile 125-mm-diameter circles of grade 3 filter papers (Whatman International) that were placed on the growth medium. Seedlings were treated with methyl viologen essentially using the strategy of Zhu et al. (39). Seedlings were grown in 150 μ mol m⁻² s⁻¹ continuous white light on sterile 125-mm-diameter circles of grade 3 filter papers (Whatman) that were placed on LS medium containing 1% sucrose for 5 d and then the filter papers were transferred to the same medium containing 1 μ M methyl viologen for 3 d. Nuclei were purified from all seedlings using the method of

Folta and Kaufman (40). Nuclear extracts were prepared by suspending nuclei in SDS-PAGE sample buffer (18) and incubating the nuclei in a boiling water bath for 5 min. After cooling to room temperature, the samples were clarified by centrifugation at $16,000 \times g$ for 10 min at 25°C. The protein concentrations of the clarified supernatants were quantified as described for whole-leaf extracts.

Cytosolic fractions were prepared as described by daSilva et al. (41) with modifications. Approximately 14 g of 7-d-old Arabidopsis seedlings that were grown on LS medium without sucrose were vacuum infiltrated and incubated with 1.5% cellulase R-10 and 0.4% macerozyme R-10 (Yakult Pharmaceutical Ind. Co. Ltd., Tokyo Japan) in TEX buffer (0.31 % Gamborg's B-5 basal salt mixture (Sigma-Aldrich), 3 mM NH₄NO₃, 400 mM sucrose, 2.6 mM MES, pH 5.7) as recommended by Estavillo et al (42). Unless indicated otherwise, the remaining steps were performed at 4°C. The protoplasts were released by repeatedly passing the digested seedlings through two layers of Miracloth (Millipore Corporation). The protoplasts were collected from the top of the filtrate after centrifuging the filtrate at $250 \times g$ for 5 min. The protoplasts were then washed three times by diluting the protoplasts with > 20 mL of TEX buffer and by centrifuging the diluted protoplasts at $250 \times g$ for 5 min. The washed protoplasts were diluted with 20 mL of 250 mM NaCl and pelleted by centrifugation at $100 \times g$ for 5 min. The pelleted protoplasts were lysed by resuspending them in extraction buffer (100 mM Tris-HCl, pH7.9, 200 mM NaCl, 1 mM EDTA, 2% β-mercaptoethanol, 10 mM Pefabloc, 33μL/mL protease inhibitor cocktail for plant cell and tissue extracts (Sigma-Aldrich), 20% glycerol and 0.2% Triton X-100). The resuspended protoplasts were incubated on ice for 10 min and then centrifuged at $21,000 \times g$ for 15 min. The protein concentrations of the supernatants (i.e., the cytosolic fractions) were determined as described for the whole-leaf extracts.

Whole-seedling extracts, nuclear fractions and cytosolic fractions were analyzed by immunoblotting (36) with anti-histone H3 antibodies (Agrisera, Vännäs Sweden), anti-UDP-glucose pyrophosphorylase antibodies (Agrisera), anti-cytosolic ascorbate peroxidase antibodies (Agrisera), anti-FtsZ1-1 antibodies, anti-FtsZ2-1 antibodies (43) or the affinity purified anti-REC1 antibodies described above. Following SDS-PAGE, all gels were electroblotted to polyvinylidene fluoride membranes. For detection of histone H3, gels were electroblotted in 25 mM CAPSO (Sigma-Aldrich), pH 10.0 and 10% methanol. For detection of REC1, gels were electroblotted in 25 mM Tris, 192 mM glycine and 0.025% SDS. For detection of FtsZ1-1 and FtsZ2-1, gels were electroblotted in 25 mM Tris, 192 mM glycine, 10% methanol and 0.005% SDS. For detection of UDP-glucose pyrophosphorylase and cytosolic ascorbate peroxidase, gels were electroblotted in 25 mM Tris, 192 mM glycine and 10% methanol. Immunoreactive bands were identified using SuperSignal West Dura Extended Duration Substrate (Thermo Fisher Scientific Inc.). The specificity of the anti-REC1 antibodies was tested by immunoblotting analysis of

wild-type and *rec1* mutant extracts as described in the text. The antibodies from Agrisera bound single bands on immunoblots. The mobilities of these bands were consistent with the masses of the proteins Agrisera claimed the antibodies bind. The specificities of the antiFtsZ1-1 and anti-FtsZ2-1 antibodies were demonstrated previously (43).

SI References

1. Ruckle ME, DeMarco SM, & Larkin RM (2007) Plastid signals remodel light signaling networks and are essential for efficient chloroplast biogenesis in *Arabidopsis*. *Plant Cell* 19:3944-3960.
2. Sessions A, *et al.* (2002) A high-throughput *Arabidopsis* reverse genetics system. *Plant Cell* 14:2985-2994.
3. Alonso JM, *et al.* (2003) Genome-wide insertional mutagenesis of *Arabidopsis thaliana*. *Science* 301:653-657.
4. Konieczny A & Ausubel FM (1993) A procedure for mapping *Arabidopsis* mutations using co-dominant ecotype-specific PCR-based markers. *Plant J* 4:403-410.
5. Adhikari ND, *et al.* (2011) GUN4-porphyrin complexes bind the ChlH/GUN5 subunit of Mg-chelatase and promote chlorophyll biosynthesis in *Arabidopsis*. *Plant Cell* 23:1449-1467.
6. Peragine A, Yoshikawa M, Wu G, Albrecht HL, & Poethig RS (2004) SGS3 and SGS2/SDE1/RDR6 are required for juvenile development and the production of *trans*-acting siRNAs in *Arabidopsis*. *Genes Dev* 18:2368-2379.
7. Barnes SA, Nishizawa NK, Quaggio RB, Whitelam GC, & Chua NH (1996) Far-red light blocks greening of *Arabidopsis* seedlings via a phytochrome A-mediated change in plastid development. *Plant Cell* 8:601-615.
8. Tamura K, *et al.* (2011) MEGA5: Molecular Evolutionary Genetics Analysis using Maximum Likelihood, Evolutionary Distance, and Maximum Parsimony Methods. *Molecular Biology and Evolution* 28:2731-2739.
9. Gasteiger E, *et al.* (2003) ExPASy: The proteomics server for in-depth protein knowledge and analysis. *Nucleic Acids Res* 31:3784-3788.
10. Dereeper A, *et al.* (2008) Phylogeny.fr: robust phylogenetic analysis for the non-specialist. *Nucleic Acids Res* 36:W465-W469.
11. Dereeper A, Audic S, Claverie JM, & Blanc G (2010) BLAST-EXPLORER helps you building datasets for phylogenetic analysis. *BMC Evol Biol* 10:8.
12. Lister C & Dean C (1993) Recombinant inbred lines for mapping RFLP and phenotypic markers in *Arabidopsis thaliana*. *Plant J* 4:745-750.
13. Bell CJ & Ecker JR (1994) Assignment of 30 microsatellite loci to the linkage map of *Arabidopsis*. *Genomics* 19:137-144.
14. Neff MM, Neff JD, Chory J, & Pepper AE (1998) dCAPS, a simple technique for the genetic analysis of single nucleotide polymorphisms: experimental applications in *Arabidopsis thaliana* genetics. *Plant J* 14:387-392.
15. Jander G, *et al.* (2002) Arabidopsis map-based cloning in the post-genome era. *Plant Physiol* 129:440-450.
16. Jez JM, Ferrer JL, Bowman ME, Dixon RA, & Noel JP (2000) Dissection of malonyl-coenzyme A decarboxylation from polyketide formation in the reaction mechanism of a plant polyketide synthase. *Biochemistry* 39:890-902.
17. Adhikari ND, Orler R, Chory J, Froehlich JE, & Larkin RM (2009) Porphyrins stabilize the association of GENOMES UNCOUPLED 4 and a Mg-chelatase subunit with chloroplast membranes. *J Biol Chem* 284:24783-24796.
18. Laemmli UK (1970) Cleavage of structural proteins during the assembly of the head of bacteriophage T4. *Nature* 227:680-685.

19. Pfaffl MW (2001) A new mathematical model for relative quantification in real-time RT-PCR. *Nucleic Acids Res* 29:e45.
20. Porra RJ, Thompson WA, & Kriedemann PE (1989) Determination of accurate extinction coefficients and simultaneous equations for assaying chlorophylls *a* and *b* extracted with four different solvents: verification of the concentration of chlorophyll standards by atomic absorption spectroscopy. *Biochim Biophys Acta* 957:384-394.
21. Rebeiz CA (2002) Analysis of intermediates and end products of the chlorophyll biosynthetic pathway. *Heme, Chlorophyll, and Bilins*, eds Smith AG & Witty M (Humana Press, Inc., Totowa), pp 111-155.
22. Schindelin J, et al. (2012) Fiji: an open-source platform for biological-image analysis. *Nat Methods* 9:676-682.
23. Fankhauser C & Casal JJ (2004) Phenotypic characterization of a photomorphogenic mutant. *Plant J* 39:747-760.
24. Serodio J, Ezequiel J, Frommlet J, Laviale M, & Lavaud J (2013) A method for the rapid generation of nonsequential light-response curves of chlorophyll fluorescence. *Plant Physiol* 163:1089-1102.
25. Müller SM, Galliardt H, Schneider J, Barisas BG, & Seidel T (2013) Quantification of Förster resonance energy transfer by monitoring sensitized emission in living plant cells. 4:413.
26. Karperien A, Ahamer H, & Jelinek HF (2013) Quantitating the subtleties of microglial morphology with fractal analysis. *Front Cell Neurosci* 7:3.
27. Karperien A (1999-2013) FracLac for ImageJ.
<http://rsb.info.nih.gov/ij/plugins/fraclac/FLHelp/Introduction.htm>.
28. Deng M, et al. (2013) Increased expression of reticulon 3 in neurons leads to reduced axonal transport of β site amyloid precursor protein-cleaving enzyme 1. *J Biol Chem* 288:30236-30245.
29. Tan K, Roberts AJ, Chonofsky M, Egan MJ, & Reck-Peterson SL (2014) A microscopy-based screen employing multiplex genome sequencing identifies cargo-specific requirements for dynein velocity. *Mol Biol Cell* 25:669-678.
30. Woo NS, et al. (2011) A mutation in the purine biosynthetic enzyme ATASE2 impacts high light signalling and acclimation responses in green and chlorotic sectors of *Arabidopsis* leaves. *Funct Plant Biol* 38:401-419.
31. Driever SM, Fryer MJ, Mullineaux PM, & Baker NR (2009) Imaging of reactive oxygen species in vivo. *Methods Mol Biol* 479:109-116.
32. Pyke KA & Leech RM (1991) Rapid image analysis screening procedure for identifying chloroplast number mutants in mesophyll cells of *Arabidopsis thaliana* (L.) Heynh. *Plant Physiol* 96:1193-1195.
33. Pyke K (2011) Analysis of plastid number, size, and distribution in *Arabidopsis* plants by light and fluorescence microscopy. *Methods Mol Biol* 774:19-32.
34. Nakagawa T, et al. (2007) Development of series of gateway binary vectors, pGWBs, for realizing efficient construction of fusion genes for plant transformation. *J Biosci Bioeng* 104:34-41.
35. Zhang X, Henriques R, Lin SS, Niu QW, & Chua NH (2006) *Agrobacterium*-mediated transformation of *Arabidopsis thaliana* using the floral dip method. *Nat Protoc* 1:641-646.
36. Harlow E & Lane D (1999) *Using Antibodies: a laboratory manual* (Cold Spring Harbor Laboratory Press, Cold Spring Harbor).
37. Sparkes IA, Runions J, Kearns A, & Hawes C (2006) Rapid, transient expression of fluorescent fusion proteins in tobacco plants and generation of stably transformed plants. *Nat Protoc* 1:2019-2025.
38. Heim DR & Larrinua IM (1989) Primary site of action of amitrole in *Arabidopsis thaliana* involves inhibition of root elongation but not of histidine or pigment biosynthesis. *Plant Physiol* 91:1226-1231.

39. Zhu J, *et al.* (2007) An enhancer mutant of *Arabidopsis salt overly sensitive 3* mediates both ion homeostasis and the oxidative stress response. *Mol Cell Biol* 27:5214-5224.
40. Folta KM & Kaufman LS (2006) Isolation of *Arabidopsis* nuclei and measurement of gene transcription rates using nuclear run-on assays. *Nat Protoc* 1:3094-3100.
41. daSilva LL, *et al.* (2005) Receptor salvage from the prevacuolar compartment is essential for efficient vacuolar protein targeting. *Plant Cell* 17:132-148.
42. Estavillo GM, *et al.* (2011) Evidence for a SAL1-PAP chloroplast retrograde pathway that functions in drought and high light signaling in *Arabidopsis*. *Plant Cell* 23:3992-4012.
43. Stokes KD, McAndrew RS, Figueiroa R, Vitha S, & Osteryoung KW (2000) Chloroplast division and morphology are differentially affected by overexpression of *FtsZ1* and *FtsZ2* genes in *Arabidopsis*. *Plant Physiol* 124:1668-1677.